

The Dynamical Evolution of Dense Rotating Systems

Paper II. Mergers and Stellar Evolution

John S. Arabadjis and Douglas O. Richstone
University of Michigan Department of Astronomy

ABSTRACT

We report the results of simulations of dense rotating stellar systems whose members suffer collisions and undergo stellar evolution processes. The initial configuration for each experiment is an isotropic Kuzmin-Kutuzov model. The dynamical evolution is simulated with the N-body tree code of Hernquist, modified to incorporate physical stellar collisions, stellar evolution, stellar mass loss and compact remnant formation, and star formation. In some simulations we have added a large accreting central black hole. In all systems the velocity dispersion in the halo evolves toward a radially biased state. In systems containing a central black hole, the dispersion becomes tangentially biased in the core, whereas it remains isotropic in systems with no black hole. Collisions tend to produce a single dominant stellar merger product, as opposed to a swarm of intermediate-mass stars. In cases where we have suppressed all processes except relaxation and physical collisions, objects with greater flattening produce larger stars through mergers. In systems where stellar ejecta are allowed to escape the system, mass loss from the heavy core stars temporarily reduces the core density and collision rate.

Most of the simulations performed reproduced the ratio of the central collision time scale to the central relaxation time scale found in the dwarf elliptical galaxy M32. The rapid central evolution of these systems due to collisions and relaxation, combined with scaling the results in N, suggests that we are either viewing M32 at a peculiar moment in its history, or that its dynamically-inferred central density is at least in part due to the present of a massive dark object, presumably a black hole.

Subject headings: Galaxy: globular clusters: general – galaxies: nuclei – galaxies: star clusters

1. Introduction

The evolution of a dense stellar system is governed by two-body relaxation, stellar evolution and mass loss, star formation, and stellar collisions. In Paper I, we examined the effects wrought by two-body relaxation, and the attendant mass segregation. This study seeks to ascertain the relative importance of the other physical processes in this list, as well as the presence of a large black hole at the system center. We simulated the evolution using the N-body tree code of Hernquist (1987, 1990), modified to include the processes listed above.

The motivation for this study is the dwarf elliptical galaxy M32, whose short core relaxation and stellar collision time scales suggest the presence of a central black hole (see Paper I for a discussion). Recent observations and dynamical modelling suggest a black hole mass of $3 \times 10^6 M_{\odot}$ (van der Marel *et al.* 1997). If M32 does not contain a black hole, it is likely that a period of wholesale stellar merging and core collapse will occur. This would result in the formation of a large black hole (Quinlan and Shapiro 1990) or a swarm of neutron stars, which could in turn collapse to form a black hole (Quinlan and Shapiro 1989). In the absence of significant heating, the primary resistance to a core collapse episode is mass mass loss from intermediate and high mass stars in the core. Applegate (1986) has shown, using a simple analytic model, that evolution of a cluster is very sensitive to the slope of the initial mass function. The results of Chernoff and Weinberg (1990) indicate that the population of Galactic globular clusters observed today may be only a subset of the primordial population, the rest having evaporated as their heaviest members shed mass and the Galactic tidal field stripped away their halos. While a much more massive system like M32 was probably never in danger of evaporating, we do expect its core evolution to be sensitive to mass loss effects.

Once gas has been liberated by a star, its fate is not clear. Whether the material should be allowed to escape the cluster or should be reprocessed into stars is an open question. Observations of M32 show little or no gas and dust (e.g. Tonry 1989), suggesting that supernovae and planetary nebulae ejecta escape the system. Supernova ejection velocities are generally far in excess of the few hundred km s^{-1} needed to escape from the core of M32. The presence of an interstellar medium undermines this argument, however. Galactic supernova remnants have been observed to sweep up 5 to 10 times their original mass (Strom 1988). Conservation of momentum would produce a corresponding reduction in speed, perhaps slowing core ejecta to sub-escape velocities. At expansion speeds of 10 to 100 km s^{-1} , planetary nebula ejecta are even more likely to be confined to the galaxy. In any case, the gas will not be swept up by the aggregate accretion of member stars. Because orbital speeds are greatly in excess of the sound speed in any ambient medium, the Bondi

accretion problem reduces to a hard-sphere crosssection (with a gravitational enhancement). The instellar medium would have to have a number density of 10^6 in order for a star to double its mass traveling at 100 km/s over 10^{10} years, far in excess of that seen in M32.

Different studies have investigated a variety of models of the evolution of the gas component. Spitzer and Saslaw (1966) created solar neighborhood type stars with their gas, while Sanders (1970) converted all ejecta into $0.5 M_{\odot}$ stars. Some have argued that material released in galactic nuclei would form massive stars (Mathews 1972, Larson 1977), while others assume that the ejecta to fall into a central black hole (David, Durisen, and Cohn 1987). In perhaps the most complete Fokker-Planck (hereafter FP) study of dense clusters to date, Quinlan and Shapiro (1990) made use of three scenarios for the destination of their liberated gas – complete system escape, reprocessing into $1 M_{\odot}$ stars, and reprocessing into stars following a Salpeter initial mass spectrum (Salpeter 1955). Because our code is strictly an N-body code, with no algorithm for treating the complex gas dynamics involved in star formation and stellar evolution processes, we have adopted two simple scenarios: in some simulations we have allowed the material to escape, and in others we have converted it to Salpeter spectrum stars.

In addition to the processes discussed above, the presence of a large black hole at the center of the system will profoundly affect the evolution of the core. Most of the work done on this problem has made use of analytic calculations and FP methods. Cohn and Kulsrud (1978) studied spherical cluster evolution using single-mass component FP calculations. Young (1980) computed analytic models wherein a pre-existing black hole grows adiabatically at the center of a spherical cluster. Lee (1992) used FP calculations to study the evolution of rotating clusters containing massive black holes in their centers. In this study we use N-body simulations to investigate the core evolution.

2. Initial simulation configuration

As described in Paper I, each of our simulations begins with an isotropic Kuzmin-Kutuzov model (hereafter KK) rotationally flattened to an ellipticity $\epsilon \in [0, 0.7]$ (Kuzmin and Kutuzov 1962; Dejonghe and De Zeeuw 1988). In some cases we have modified the potential-density pair to include a central black hole. Defining M_{\bullet} and M as the black hole mass and total mass, respectively, the potential-density pair becomes

$$\phi(\varpi, z) = -\frac{G(M - M_{\bullet})}{(\varpi^2 + z^2 + a^2 + c^2 + 2\sqrt{a^2c^2 + c^2\varpi^2 + a^2z^2})^{1/2}} - \frac{GM_{\bullet}}{(\varpi^2 + z^2)^{1/2}} \quad (1)$$

and

$$\rho(\varpi, z) = \frac{(M - M_{\bullet})c^2}{4\pi} \left[\frac{(a^2 + c^2)\varpi^2 + 2a^2z^2 + 2a^2c^2 + a^4 + 3a^2\sqrt{a^2c^2 + c^2\varpi^2 + a^2z^2}}{(a^2c^2 + c^2\varpi^2 + a^2z^2)^{3/2}(\varpi^2 + z^2 + a^2 + c^2 + 2\sqrt{a^2c^2 + c^2\varpi^2 + a^2z^2})^{3/2}} \right] + \frac{M_{\bullet}\delta(0)}{4\pi}. \quad (2)$$

Here ϖ , z , and ϕ are the usual cylindrical coordinates, and c and a are scale lengths, with c/a roughly corresponding to the model’s axial ratio (Dejonghe and De Zeeuw 1988). As discussed in Paper I, the particle velocities are obtained with the (modified) KK density/potential pair and the Jeans equations under the assumption of isotropy (Satoh 1980; Binney *et al.* 1990). The initial stellar coordinates are sampled according to the prescription laid out in Paper I. The initial equilibrium of systems created in this way is demonstrated in Figures 1 and 2. The former shows the core region of a black hole model at $t/t_{rc} = 0, 1, 2$, and 3, while the latter shows the same but in velocity space. The black hole is represented by a filled circle near the origin. There is little evolution over the first few local relaxation times, indicating that the system is very much in equilibrium.

The mass spectrum used for each simulation is either a delta function or a Salpeter spectrum. For the simulations which use the Salpeter IMF we use $m_{min} = 0.2 M_{\odot}$, rather than the standard $0.08 M_{\odot}$ (e.g. Grossman, Hays, and Graboske 1974), in order to populate the top decade of the distribution for $N=3000$ (see discussion in Paper I). We set $m_{max} = 100 M_{\odot}$ for some our models (Humphreys and Davidson 1986), but for others we use $1 M_{\odot}$, since more massive stars would have perished by now, given an age of 10^{10} y for M32.

3. Physical Processes

The physical processes which dominate the evolution of a dense stellar system are two-body gravitational relaxation, stellar evolution and mass loss, gas dynamics and star formation, stellar collisions, binary star interactions, and external tidal fields. In the case where the cluster contains a central massive black hole, tidal disruption of low- J stars will also affect the cluster structure.

As discussed in Paper I, binary stars will not significantly alter the evolution of the core of M32, and so they are not included in these simulations. Tidal fields may strip

members from the outer halo of M32; however, these simulations are geared primarily to investigate the core of M32, and so we ignore tidal stripping.

3.1. Two-body Relaxation

The dynamical evolution of these systems was simulated using the N-body tree code of Hernquist (1987, 1990), a FORTRAN implementation of the Barnes and Hut (1986) hierarchical force algorithm. Two-body relaxation is the scattering of stars off irregularities in the gravitational field of the galaxy due to the finite number of stars. The time scale associated with this process is given by (e.g. Binney and Tremaine 1987, hereafter BT)

$$t_{\text{rc}} = 0.337 \frac{\sigma^3}{G m_{\star} \rho \log \Lambda}. \quad (3)$$

Here ρ is the stellar density, σ is the velocity dispersion, m_{\star} is the stellar mass, and $\log \Lambda$ is the Coulomb logarithm. Relaxation dominates the evolution of dense systems whose stars have a range of masses (Spitzer and Saslaw 1966; Hénon 1975; Chernoff and Weinberg 1990; Giersz and Heggie 1996), but even for systems with stars of equal mass relaxation will be extremely important because stellar collisions will produce and subsequently flatten a mass spectrum.

3.2. Stellar Evolution and Mass Loss

Roughly 90% of a star’s life is spent on the main sequence (Iben 1964), and so in all of our simulations we assume that a star will remain on the main sequence until it sheds mass and becomes a compact remnant. We adopt a power law for the main sequence mass-radius relation:

$$\frac{r}{R_{\odot}} = \left(\frac{m}{M_{\odot}} \right)^{\beta}. \quad (4)$$

For low-mass ($0.1 < m < 2 M_{\odot}$) main sequence stars, β is about 0.55 (Iben 1964; Bond, Arnett, and Carr 1984). A stellar merger event would probably produce a star which is temporarily bloated; however, since the Kelvin-Helmoltz time scale (the time required for the bloated star to settle down onto the main sequence) is much shorter than the collision time scale in our simulations, we do not need to modify the mass-radius relation (see, e.g.,

Quinlan and Shapiro 1990).

We calculate the stellar lifetime from a parabolic fit to the data in Iben (1964). We adopt

$$(\tau - \tau_0) = \beta(\mu - \mu_0)^2 \quad (5)$$

for $m \leq 100 M_\odot$ and $\tau = \text{constant}$ for $m \geq 100 M_\odot$, where $\mu = \log_{10}(m/M_\odot)$ and $\tau = \log_{10}(t/10^6\text{y})$. Since the mass-to-light ratio approaches a constant as m increases, due to the Eddington limit, we require that

$$\lim_{m \rightarrow 100 M_\odot} \frac{d\tau}{d\mu} = 0 . \quad (6)$$

The parameters chosen were $\mu_0 = 2$, $\tau_0 = 0.5$, and $\beta = 0.87$. For $m > 100 M_\odot$ we set $\tau = \tau_0$, which corresponds to a lifetime of 3.16 My. The Iben data and the parabolic fit are shown in Figure 3.

A star spends 90% of its life on the main sequence, or near enough to it that its radius has not changed appreciably (Iben 1964, 1967). For this reason, and because giants have extremely tenuous atmospheres, stars in all of our models are considered to be on the main sequence until a mass-loss event at their death, for purposes of calculating their collision cross section. Reimers and Koester (1982) have argued that stars of $m < 8 M_\odot$ will leave behind white dwarfs as their stellar evolution remnant, although stars in the upper part of this range could explode as carbon-detonation supernovae, leaving no remnant (see Iben and Renzini 1983 for review). We choose to assign white dwarf remnants to these stars. Since the white dwarf mass distribution is strongly peaked at $0.6 M_\odot$ (Weidemann 1990), we use this value as our remnant mass. The rest of the stellar material is either ejected from the cluster on a very short time scale, or it is reprocessed into stars, depending on the model. The stars created from ejecta are assigned coordinates according to the initial $(m, \mathbf{x}, \mathbf{v})$ distribution.

Bethe (1986) has argued that stars with masses $8 \leq m < 25 M_\odot$ die in supernova explosions, leaving neutron star remnants, while stars of mass $m > 25 M_\odot$ produce black hole remnants. We adopt this view (because it is simple) and set all neutron star masses to $1.4 M_\odot$, consistent with binary pulsar measurements (Hulse and Taylor 1975, Taylor and Dewey 1988, Taylor and Weisberg 1989). The theoretical upper limit for the neutron star mass is about $3 M_\odot$; it is somewhat less when more elastic (realistic) equations of state are assumed (Chitre and Hartle 1976). Several observed binary systems show companions

whose masses exceed this limit, suggesting the presence of a black hole (for a review see Cowley 1992). The four most robust stellar-mass black hole candidates are listed in Table 1. In our simulations we set the remnant black hole mass equal to $0.2m M_{\odot}$, producing holes with masses $\geq 5 M_{\odot}$, with the remaining mass ejected as a supernova explosion (Bodenheimer and Woosley 1983; Woosley and Weaver 1986).

3.3. Star Formation

As mentioned previously, our simulations utilized two procedures for treating mass ejecta. For the simulations in which ejected material is converted into stars, the stellar masses and positions were assigned according to the prescription described in Paper I. At the end of each time step during which there was at least one mass loss event, the ejecta are pooled together. After as many stars on the appropriate mass interval have been formed, the remaining material is assigned to a single star on the interval $(0, 0.2] M_{\odot}$.

3.4. Stellar Collisions

The mean time for a star of radius r_{\star} and mass m to suffer a physical collision with another star in a stellar system with number density n and dispersion σ is given by (BT)

$$t_{\text{coll}} = [16\sqrt{\pi}n\sigma r_{\star}^2(1 + \Theta)]^{-1}. \quad (7)$$

Recent observations (van der Marel *et al.* 1997) show that the central velocity dispersion of M32 $\sigma_0 = 126 \text{ km s}^{-1}$. A stellar collision in this range would most likely result in the merging of the two stars, with little mass loss, for a wide range of stellar masses (Benz and Hills 1987, 1992; Lai, Rasio, and Shapiro 1993). Thus we assume that stellar collisions in the core of M32 result in merger events, with no mass loss.

Figure 4 shows collision and relaxation time scale contours for a wide range of velocity dispersion and density. The core properties of a few stellar systems are also shown. The solid symbols assume that the core consists of main sequence stars only – there would be a moderate collision rate enhancement for cores containing a significant fraction of binary stars. The open symbol for M87 uses the observed central star light density ($5000 L_{\odot} \text{ pc}^{-3}$); the closed symbol assumes that the inferred mass density is due solely to the presence of $1 M_{\odot}$ stars. (This is clearly not the case – it has been known for decades that the nucleus of M87 is quite active.) The open symbol for M32 evaluates the cusp model of Lauer *et al.*

(1992) at $r = 0.1$ pc and the solid symbol represents the 0.37 pc core model of the same study.

A study of the effects of stellar collisions on dynamical evolution would naturally focus on those systems found to the right of the $t_{col} = 10$ Gy contour. As this figure suggests, globular clusters generally do not possess the core properties required for stellar collisions to be important. The exception to this is NGC 6256, whose high central density and low dispersion make it an interesting laboratory for studying the effects of collisions. Globular cluster evolution can be strongly influenced by the presence of binary stars, however. Since the tree code is not equipped to handle binaries we have restricted our study to M32.

3.5. Central black hole accretion

Collisions of stars with a central black hole are treated in a different fashion. We assume that stars which venture too close to the hole are disrupted by tidal forces. If \mathbf{x}_\star and \mathbf{x}_\bullet are the star and black hole positions, respectively, then tidal disruption occurs if

$$|\mathbf{x}_\star - \mathbf{x}_\bullet| \leq r_\star \left(\frac{3M_\bullet}{m_\star} \right)^{1/3}. \quad (8)$$

Thus there are three relevant mass parameters for the system: M_\bullet/M_{total} , m_\star/M_\bullet , and m_\star/M_{total} . Due to the necessity of simulating M32 with far fewer stars than it actually contains, we cannot preserve all three of these ratios simultaneously. At this point it is not feasible to simulate M32 with an N-body code using $N=10^8$, so we seek only to preserve the first two of these ratios. First, we seek to simulate only the inner 10% of the system so that M_{total} is a tenth of the actual system mass. Using M32 as our guide (e.g. van der Marel 1997), we set $M_\bullet/M_{total}=0.1$. The M_\bullet in equation 8 is in essence a free parameter, unrelated to M_\bullet/M_{total} . Thus we set $M_\bullet/m_\star = 10^6$ in order to characterize the tidal disruption and black hole accretion properly.

4. The Models

The effects of stellar collisions on the dynamical evolution of dense systems are quite tangled. On the one hand, collisions will tend to produce a high density core. Heavy stars formed through mergers will sink to the center of the system as they attempt to come to energy equipartition with the surroundings. In addition, the completely inelastic merging of a pair of unbound stars removes energy from the system, which in turn deepens the central

potential (and mass density). For a monotonically increasing mass-radius relation for main sequence stars, as orbits of heavy stars decay, their increasing cross section and density will enhance the frequency of collisions. In the absence of other processes a single high mass star may form, merging with all others which migrate to the core.

On the other hand, collisions in the core can help indirectly to terminate the infall of heavy stars. High mass stars are short-lived, and if the collision time scale exceeds the stellar evolution time scale, mass loss tends to remove material from the core, even if it does not escape the system as a whole. This makes the central potential more shallow, and the core, no longer in virial equilibrium, begins to expand.

In order to discriminate among these effects we sought first to understand the influence of stellar collisions on system evolution, in the absence of mass loss. In particular, we wanted to know if the collision process favored the formation of a single stellar merger remnant or a swarm of intermediate mass objects, for a ratio of relaxation and collision time scales found in astronomical objects. We designed the input models such that $t_{col}/t_{rel} \simeq 100$, as in the case in the core of M32. We also wanted to know if the flatness of the system influences the collision rate or the mass of the merger remnants. We performed eight simulations of 300 bodies each (Group 1). The input models varied in initial flatness from $c/a = 1.0$ to 0.3, roughly corresponding to axisymmetric elliptical galaxies E0 through E7, respectively.

The next set of experiments we ran (Group 2) were designed to explore the effect of mass loss and stellar collisions on system evolution, as well as the influence of a central black hole. We decided to run four simulations of 3000 bodies each, two with a central black hole (using $M_{\bullet}=0.1M$, similar to a possible nuclear configuration of M32) and two without black holes. Since we were interested in rotation effects, we ran each with $c/a = 1.0$ and 0.3. We opted to use equal-mass stars in the input models to reduce the noise associated with a mass spectrum. This also allows us to compare the black hole results with analytic models in the literature.

The last group of experiments we performed (Group 3) were specifically designed to mimic as many of the characteristics of M32 that our dynamic range would allow. We set $c/a = 0.8$, $t_{col}/t_{rel} = 100$, and we used a Salpeter spectrum for the initial mass function. We looked at the effect of star formation (recycling of stellar ejecta) on the core structure and the N dependence of the results.

Table 2 summarizes the model parameters for each of the simulations. In the second column a and c are the relevant scale lengths in the KK model. Column 3 lists the initial number of bodies in each simulation, and column 4 indicates the mass spectrum used. The stellar mass range is given in column 5, and columns 6-8 indicate which astrophysical

processes (stellar evolution, physical stellar collisions, and star formation, respectively) were incorporated in each simulation. The ratio of the collision time scale to the relaxation time scale for the core is given in column 9, and the central black hole mass is listed in column 10.

The last model listed under Group 3 (model XVIII) was not designed to reproduce the probable ratio of the collision to relaxation time scales in M32. Rather, the simulation was performed to examine the types of stellar remnants produced for a value of t_{col}/t_{rel} which, although it is unlikely value for the unresolved core of M32, is still a plausible value for some dense stellar systems.

4.1. Stellar Collisions and Merger Remnants

We first examined the collision process in absence of all other physical processes except relaxation. We ran eight simulations (Group 1) for 100 half-mass relaxation times, with $t_{ch}/t_{rh} = 100$. We varied c/a along the sequence, ranging from 1.0 through 0.3 (corresponding to E0 through E7).

Because $t_{rh} \ll t_{ch}$ and $t_{rh} \ll t_{evo}$ ($t_{evo} \equiv \infty$ for this set of experiments), each merger remnant will fall to the center before it collides again. Therefore when they do collide a second time they are more likely to collide with another merger remnant, since the core of the system will be populated with the heaviest stars. This effect is shown in Figure 5, which shows the location of collision events in the spherical case (model XVIa) versus time. Events marked with an ‘x’ denote collisions between $1 M_{\odot}$ stars, and triangles represent collisions between stars whose masses sum to $10 M_{\odot}$ or less (but greater than $2 M_{\odot}$). Circles denote collisions between stars whose mass sum is greater than $10 M_{\odot}$; this last category amounts to collisions between field stars and the dominant merger remnant. Open circles represent collisions of $1 M_{\odot}$ stars with the merger remnant, and filled circles are collisions between the dominant remnant and heavier stars. Collisions between $1 M_{\odot}$ stars occur over a much wider range than collisions between heavier stars. Collisions between intermediate mass stars occur during a short phase near $t = 100$, after which the dominant merger remnant is a participant in most of the collision events. The collision evolution in the more flattened systems follows the same pattern.

The mass of the merger remnant appears to be mildly dependent upon the rotational state, with flatter systems producing somewhat larger dominant merger remnant. The mass of the next largest (secondary) star appears to be independent of the flattening. The merger remnant and secondary star masses at simulation termination are shown in Figure 6.

The reason for the the rotational dependence of the collision process can be traced to the early evolution of the core. It is well known that if the characteristic rotation speed is too large, the system is unstable to $l=2, m=2$ modes (ellipsoidal “bar” structures). Kalnajs (1972) and Ostriker and Peebles (1973) showed that the criterion for stability against the formation of bar modes can be written

$$\frac{T}{|W|} < t_{crit}, \quad (9)$$

Here T is the kinetic energy associated with the rotation and W is the potential energy. Kalnajs (1972) showed analytically that, for a certain class of disk models which bear his name, $t_{crit} = 125/486 = 0.1286$. Ostriker and Peebles (1973) used N-body simulations of Mestel disks to derive $t_{crit} \simeq 0.14$. $T/W \simeq 0.16$ at $t = 0$ in our E7 KK model (XVIIh), indicating that it is bar-mode unstable. In Figure 7 we show the evolution of $T/|W|$ for the this model. The system quickly forms a bar structure which transports angular momentum outward, allowing the core to contract more rapidly and driving up the central density. The bar cannot be seen simply by viewing the system from above, due to the low number of bodies. It can be seen, however, by comparing the mass of stars in each quadrant (I–IV) as the cartesian axes are rotated by an amount $\delta\phi$. If the system is indeed centered on the origin, and a true bar structure exists, then the quantity $(m_I + m_{III}/m_{II} + m_{IV})$ should show be sinusoidal in the variable $\delta\phi$ (Fig. 8). Figure 9 shows this quantity for model XVIIh, clearly demonstrating the existence of a bar.

The increase in the density enhances the collision rate, which in turn builds up the dominant merger remnant. It is impossible to distinguish between the two processes – core contraction and stellar mergers – since they enhance each other. Their influence can be observed in their effect on the density profile. The density of the two extreme cases, $c/a = 1.0, 0.3$, is shown at three different times in Figure 10. The dominant merger remnant is found within the innermost data point in each plot.

The increased central density allows the flatter rotating model to experience its collision phase earlier in its evolution than a more spherical model. Figure 11 shows the collision rate for the two extreme cases. Both systems experience an episode of enhanced collision activity; that of the flattened system comes at a slightly earlier time, however, because of the more rapid increase in the core density. Relaxation causes the core of a system to shrink in mass as well as size; since collisions occur in the core, the earlier the episode occurs, the more stars available for merging.

Under the conditions explored in these simulations, with $t_{col}/t_{rel} = 100$, only one experiment produced a compact remnant other than a white dwarf. (Model XII produced

a neutron star in the vicinity of the central black hole.) This is not due to the physical conditions present, although it is true that if the Salpeter systems with masses on the range $[0.2,100] M_{\odot}$ were allowed to undergo stellar evolution processes, we would likely produce a black hole or two and many neutron stars, since there would be many stars with the requisite initial mass. The failure of these simulations to produce neutron stars and black holes is simply due to the limited dynamic range of the simulations. Because of time constraints, we were forced into the trade-off between the number of stars in a simulation and the number of simulations. We settled on a low N so that we could explore a range of parameters relevant to dense elliptical galaxies. One effect of low N is to directly limit the mass of the dominant merger remnant. Obviously a system of mass M cannot form a remnant with a mass exceeding M . If a system is allowed to evolve for a period equal to its half-mass collision time scale, one might expect that the merger remnant mass m_{rem} would be some fraction of the total number of stars available to the collision process, $N/2$. We therefore write

$$m_{rem} = \epsilon \frac{N}{2}, \quad (10)$$

where ϵ is an efficiency which depends on at least three quantities – the stellar evolution, relaxation, and collision time scales. From our Group 2 simulations we can estimate ϵ in the case where the stellar evolution time scale is infinite. The largest stellar mass to form was made from 29% of the $N/2$ particles nominally available for merging. When stellar evolution effects are included, the efficiency suffers dramatically.

The dominant merger remnant produced in some of the simulations is listed in Table 3. In Figure 12 we plot the merger efficiency versus the number of stars in the system for XIII and XV. The points appear to follow a power law with a slope of about -0.7. In the absence of any new astrophysical processes becoming important on the interval $3 \times 10^3 < N < 10^8$, two interesting mass scales become apparent. In order for a system to produce a black hole through stellar collisions, the quantity $\epsilon N/2$ must equal or exceed $25M_{\odot}$. The minimum N required to do this is about 2×10^6 . This value exceeds most globular cluster masses, suggesting that globular clusters are not able to form black holes in their cores through stellar mergers. For a system with $N=3 \times 10^8$, a star of mass $100 M_{\odot}$ can be produced through collisions, consistent with the results of Quinlan and Shapiro (1989).

As an alternative to increasing N (or scaling N through a power law fit) to produce a central black hole through stellar collisions is to reduce t_{ch}/t_{rh} . If we have an unresolved galaxy core like M32 (Lauer *et al.* 1992), it is possible (though unlikely – see, e.g., Goodman and Lee 1989) that the true central number density is much larger than the lower limit

we are able to assign. In that case, if we scale up the density, we scale up the age of the galaxy, measured in units of the collision time scale. Unfortunately, the relaxation time scales with density roughly as does the collision time; the ratio does not change. However, in the regime of non-disruptive stellar collisions,

$$t_{ch}/t_{rh} \propto \sigma^{-2}. \quad (11)$$

If the central dispersion of M32 were a factor of 3 higher than current observations suggest (again unlikely), then we could reduce the ratio to 10 from 100. While this is probably not realistic for M32, it may be for other systems. With this in mind, we ran an additional simulation (model XVIII) which set $t_{ch}/t_{rh} = 10$, but which in all other respects conformed to the parameters of model XV.

Between $t = 0$ and $100t_{dh}$ the core collision rate is about 4 collisions per t_{dh} . At $t = 100t_{dh}$, two black holes are formed ($m=10.6, 6.2 M_{\odot}$); accompanying this is the shedding of $67.2 M_{\odot}$ of material, which is 6% of the total mass. Although this material is reprocessed into stars, it is lost, at least temporarily, from the core, dramatically reducing the core density and collision rate. In addition to the pair of black holes, the system produced nine neutron stars, four white dwarfs, and an additional 553 main sequence stars from recycled ejecta. The merger efficiency for this system was about 5%. While the simulation may have little relevance to M32, it is nonetheless interesting that large objects can be produced through merger events with only a moderate, and plausible, adjustment to the model parameters, even within a low N system.

4.2. Central Black Hole Models

Next we contrast the evolution of systems which do or do not contain black holes in their nuclei. We expect that the density profiles of the core of each system would show evidence of a massive object within the black hole “cusp radius”, defined by

$$r_{cusp} = \frac{GM_{\bullet}}{\sigma^2}, \quad (12)$$

Cohn and Kulsrud (1978) used Fokker-Planck calculations of spherical clusters to derive an $r^{-7/4}$ density profile. Young (1980) modeled a spherical cluster containing a central black hole under the assumption that the black hole grows adiabatically. He found that the density profile goes as $r^{-3/2}$ for a completely isotropic core and $r^{-9/4}$ for a core whose stars all lie on circular orbits. More recently, Quinlan *et al.* (1995) calculated models for black

holes in spherical clusters, and derived similar results. They found that $\rho \sim r^{-3/2}$ near the black hole in a model whose core initially resembles an isothermal sphere. The system retained an isotropic velocity dispersion near the black hole; a tangential bias was seen in the dispersion away from the hole. For their non-isothermal models, they found that the density cusp was steeper, and that the anisotropy penetrated right into the center.

In Figure 13 we show the density profiles for our simulations which contain a central black hole and equal-mass stars. We fitted a power law of slope α to the inner 15% of each system (neglecting the innermost point containing the black hole), which falls within the black hole cusp radius. The data points used in the power law fit are shown as circles or triangles in each graph. (In each case $r_{cusp} \simeq 2.5$.) For the spherical system (model XI) we found that $\alpha = -1.79 \pm 0.08$; the flattened system (XII) had a slightly steeper profile at $\alpha = -2.15 \pm 0.06$. The initial and final profiles of model XI are shown in Figure 14 to demonstrate the evolution from a core-like to a cusp-like profile.

Next we show the density profile for four models with a Salpeter IMF and rotationally flattened to $c/a = 0.8$. The first two (models XIIIa and XVII, Figure 15) contain no central black hole. Model XVII, which evolves under the influence of two-body relaxation only, has a somewhat more shallow core profile than does model XIIIa, which incorporates stellar evolution and collisions. This is due to the fact that stellar collisions produce a flatter effective mass function, and the subsequent mass segregation moves heavier stars into and lighter stars out of the core, increasing the density gradient. The simulations of Figure 16 each contain a black hole of mass $M_{\bullet}/M_{\odot}=0.1$. Model XIVa, which incorporates stellar evolution (mass loss) and merging, has a steeper core profile, again due to the effects of mass segregation. In simulations which evolve under the influence of relaxation only (XVII and XIVb), the system which contains a black hole (XIVb) develops a steeper core profile. As in the case without central black holes, the system which allows stellar collisions and evolution produces a steeper profile than the system which does not.

Models with and without central black holes show a marked difference in the behavior of their velocity dispersions. Each of the simulations started with isotropic dispersions; relaxation and mergers drive the systems away from isotropy.

We plot the dispersion ratios σ_{θ}/σ_r and σ_{ϕ}/σ_r for each Lagrangian quintile of the models which contain no central black hole, in Figure 17. (The curves have been smoothed over three bins.) These systems tend to preserve an isotropic dispersion in their cores, while their halo dispersions become radially biased outside the half-mass radius.

The spherical black hole model (XI), on the other hand, develops a strong tangential bias. In Figure 18 we do not plot the innermost quintile because it is quite noisy due to

the fact that this mass quintile initially houses the black hole, and eventually *becomes* the black hole when the hole mass reaches 0.2 through accretion. In the rotating black hole model ($c/a = 0.3$, model XII), the core of the system appears to remain isotropic. The reason for this is unclear. It is not related to the similar finding of Quinlan *et al.* – their system behaved in such a way due to an isothermal initial core structure, in contrast to their non-isothermal core model. In our systems, however, the cores start off identically; they both possess isotropic cores, with only the flattening differing between the two. The plummeting dispersion ratio of the outermost Lagrangian quintile is due to the presence of stars which have escaped the system.

4.3. M32 Simulations

The simulations of Group 3 were specifically designed to mimic the evolution of M32. Assuming that M32 is 10 Gy old, we simulated it with a Salpeter spectrum with $m_{max} = 1.0 M_{\odot}$, since presumably stars with masses greater than $1 M_{\odot}$ (neglecting blue stragglers formed through collisions) would have perished by now. (We note, however, that there is some evidence for the the presence of a 5 Gy old population – see Freedman 1989.) We scaled the stellar radii to produce a time scale ratio $t_{col}/t_{rel} = 100$.

An important issue when simulating M32 is to understand how the decision to treat mass loss from the stars affects the outcome of experiments. As it turns out, the recycling of stellar ejecta into new stars does not have a straightforward effect on the evolution of the core. One might expect that star formation would simply prevent the core from evaporating as heavy stars therein shed mass. The picture is somewhat more complicated.

Initially, mass recycling does prolong the episode of core contraction (Figure 19). The core density of a recycling model continues to rise past the point where the non-recycling system begins to expand. However, the increased amount of material in the core results in a larger average stellar mass in the core. These larger stars lose proportionately more mass when they become white dwarfs, and the net effect is that the core density will be *lower* when mass ejecta are recycled into stars, for a period of time equal to that during which it was higher (Figure 20). After 100 relaxation times, or about 2800 dynamical times, the recycling system density again exceeds the non-recycling density. This corresponds to about 10^{10} years, indicating that the present core density of an elliptical galaxy cannot be used to determine whether mass loss from stars in the core escapes the system.

The FP calculations of Lee (1992) showed that the rotation parameter V/σ increases as one moves in toward the center of a system with an empty loss cone (i.e. maximally

accreting) black hole. He found that the rotation speed increases all the way in to the core, and that the velocity dispersion is “Keplerian” (i.e. $\sigma \sim r^{-1/2}$) over the inner region. Our simulations concur with two of these conclusions. In Figure 21 we show V , σ , and V/σ versus radius for four different times in the simulation XII. While the dispersion falls as $r^{-1/2}$, and the rotation speed rises into the center, the behavior of V/σ is not clear. It appears that the slope of V/σ is increasing as the system evolves, but whether or not it would evolve to the stage where it rises all the way in to the center is unknown. We concur with Lee’s result that V/σ fails to rise inward for black hole systems with no loss cone. However, we found that V/σ fails to rise inward for the mildly rotating model XIVa. It is possible that this is a result of limited dynamic range. While M_{\bullet}/m_{\star} was *set* to 10^6 for the process of black hole accretion, it is only around 300 *gravitationally*, so rotation speeds near the hole are lower than they would be in a system with $N=10^6$. If this is indeed the problem, there is no clear way around it except for increasing N considerably beyond the range $30 \leq N \leq 3000$ explored in this study.

5. Conclusions

Several important pieces of information can be extracted from the simulations performed in this study. The first is that a system with the same time scale ratio t_{ch}/t_{rh} and flattening as M32 has a strong tendency to evolve away from its initial configuration through stellar merger events and two-body relaxation. Specifically, such a system would rapidly build up a considerably flatter stellar mass spectrum in the core. Another is that the dominant merger remnant mass for (physically) collisional systems increases with increasing N . Finally, the decision of whether or not to recycle mass ejecta into stars does not significantly change these trends, although it does alter the evolution of the core structure. Taken together, these points suggest that M32 harbors a black hole in its nucleus. If the nucleus of M32 contained no central black hole, these simulations show that it would evolve away from this state rather rapidly. If the core were composed of stars, physical stellar collisions would produce a steeper core density profile by flattening the stellar mass spectrum. In addition, these collisions would tend to produce a single dominant merger remnant, further changing the core structure. If the core were a cluster of compact objects, energy losses by gravitational radiation might result in mergers and core collapse (Quinlan and Shapiro 1989). Goodman and Lee (1989) put a lower limit of 0."1 on the half-mass radius of any embedded dark cluster, while van der Marel *et al.* (1997) have ruled out dark clusters with a Plummer scale length greater than 0."06. In either case, our present view of M32 would be of a special point in its history, at the threshold of an epoch of intense nuclear activity. The third scenario, in which the central mass concentration is in the form

of a black hole, would result in a less rapid central evolution, and thus would not invoke an assumption of our observations being conducted during a special time period.

An extrapolation of the results of these numerical experiments suggest that globular clusters are probably incapable of forming black holes through stellar collisions, whereas a larger system like M32 can form a $100 M_{\odot}$ black hole, consistent with Quinlan and Shapiro (1989). Once formed, all subsequent collisions serve only to increase the black hole mass, and thus the black hole formed in this manner can provide the seed required in many models of active galactic nuclei.

Our simulations concur with the Fokker-Planck of Cohn and Kulsrud (1978) with regard to the density profile $\rho \propto r^{\alpha}$ in the vicinity of a central black hole. For spherical clusters we find that $\alpha = -1.79 \pm 0.08$, consistent with the Cohn and Kulsrud value of -1.75, for systems containing equal-mass stars. Furthermore, we show that the profile steepens somewhat for rotationally flattened systems, and significantly for systems following a Salpeter mass spectrum. In systems containing a black hole, a Salpeter mass spectrum, stellar collisions and stellar evolution, we find $\alpha = -2.88 \pm 0.16$.

Future work along these lines can be conducted according to two different guiding principles. One of these need hardly be stated: to improve the statistics and the dynamic range, one should increase the number of particles. It is essential that the scaling of dominant merger remnant mass with N be fully understood to extrapolate these results in a more quantitative fashion to elliptical galaxies. Performing these experiments with 10^4 and 10^5 particles would produce a more robust scaling relation. One would also like to verify the minimum value of N derived in this study for which a system described by $t_{col}/t_{rel} = 100$ will produce a large black hole through stellar mergers. The second approach is to combine the results of N_s experiments which differ only in the random variables used to generate the stellar distribution function (Giersz and Heggie 1994, 1996). The results can then be combined in an appropriate manner to extract a higher signal-to-noise ratio. With increased N or N_s one can construct distribution functions in E and L_z which are much more smooth than the current study would produce. This would facilitate more detailed and quantitative comparisons with FP results.

This research was supported by NASA Theory Grant NAG 5-2758. DR thanks the J. S. Guggenheim Foundation for a fellowship and the Ambrose Monell Foundation for support.

REFERENCES

- Applegate, J. H. 1986, *Ap. J.*, **301**, 132.
- Barnes, J., and Hut, P. 1986, *Nature*, **324**, 446.
- Benz, W., and Hills, J. G. 1992, *Ap. J.*, **389**, 546.
- Benz, W., and Hills, J. G. 1987, *Ap. J.*, **323**, 614.
- Bethe, H. A. 1986, in *Highlights of Modern Astrophysics*, ed. S. L. Shapiro and S. A. Teukolsky (New York: Wiley), p. 45.
- Binney, J. J., Davies, R. L., and Illingworth, G. D. 1990, *Ap. J.* **361**, 78.
- Binney, J. J., and Tremaine, S. 1987, *Galactic Dynamics* (Princeton: Princeton University Press).
- Bodenheimer, P., and Woosley, S. E. 1983, *Ap. J.*, **269**, 281.
- Bond, J. R., Arnett, W. D., and Carr, B. J. 1984, *Ap. J.*, **280**, 825.
- Chernoff, D. F., and Weinberg, M. D. 1990, *Ap. J.*, **351**, 121.
- Chitre, D. M., and Hartle, J.B. 1976, *Ap. J.*, **207**, 592.
- Cohn, H. N., and Kulsrud, R. M. 1978, *Ap. J.* **226**, 1087.
- Cowley, A. P. 1992, *Ann. Rev. Astron. Astrophys.*, **30**, 287.
- David, L. P., Durisen, R. H., and Cohn, H. N. 1987, *Ap. J.*, **316**, 505.
- Dejonghe, H., and De Zeeuw, T. 1988, *Ap. J.*, **333**, 90.
- Freedman, W. L. 1989, *Astron. J.*, **98**, 1285.
- Giersz, M., and Heggie, C. D. 1994, *M. N. R. A. S.*, **268**, 257.
- Giersz, M., and Heggie, C. D. 1996, *M. N. R. A. S.*, **279**, 1037.
- Goodman, J. and Lee, H. M. 1989 *Ap. J.*, **337**, 84.
- Grossman, A. S., Hays, D., and Graboske, H. C. 1974, *Astron. Astrophys.*, **30**, 95.
- Hénon, M. 1975, in *IAU Symp. No. 69, Dynamics of Stellar Systems*, ed. A. Hayli (D. Reidel Publishing Company, Dordrecht), p. 133.
- Hernquist, L. 1987, *Ap. J. Supp. Ser.*, **64**, 715.
- Hernquist, L. 1990, *J. Comp. Phys.*, **87**, 137.
- Hulse, R. A., Taylor, J. H. 1975, *Ap. J. Lett.*, **195**, L51.

- Humphreys, R. M., and Davidson, K. 1986, *New Scientist*, **112**, 38.
- Iben, I. 1964, *Ap. J.*, **140**, 1631.
- Iben, I. 1967, *Ap. J.*, **147**, 624.
- Iben, I., and Renzini, A. 1983, *Ann. Rev. Astron. Astrophys.*, **21**, 271.
- Kalnajs, A. J. 1972, *Ap. J.*, **175**, 63.
- Kippenhahn, R., and Weigert, A. 1990, *Stellar Structure and Evolution* (New York: Springer-Verlag).
- Kuzmin, G. G., and Kutuzov, S. A. 1962, *Bull. Abastumani Ap. Obs.*, **27**, 82.
- Lai, D., Rasio, F. A., and Shapiro, S. L. 1993, *Ap. J.*, **412**, 593.
- Larson, R. B. 1977, in *The Evolution of Galaxies and Stellar Populations*, ed. B. M. Tinsley and R. B. Larson (New Haven: Yale University Observatory), p. 97.
- Lauer, T., Faber, S. M., Lynds, C. R., Baum, W. A., Ewald, S. P., Groth, E. J., Hester, J. J., Holtzman, J. A., Kristian, J., and Light, R. M. 1992, *Astron. J.*, **103**, 703.
- Lee, M. H. 1992, Ph.D. Thesis, Princeton University.
- Mathews, W. G. 1972, *Ap. J.*, **174**, 101.
- Ostriker, J. P., and Peebles, P. J. E. 1973, *Ap. J.*, **186**, 467.
- Quinlan, G. D., Hernquist, L., and Sigurdsson, S. 1995, *Ap. J.*, **440**, 554.
- Quinlan, G. D., and Shapiro, S. L. 1990, *Ap. J.*, **356**, 483.
- Quinlan, G. D., and Shapiro, S. L. 1989, *Ap. J.*, **343**, 725.
- Reimers, D., and Koester, D. 1982, *Astron. Astrophys.*, **116**, 341.
- Richstone, D. O., Bower, G., and Dressler, A. 1990, *Ap. J.*, **353**, 118.
- Salpeter, E. E. 1955, *Ap. J.*, **121**, 161.
- Sanders, R. H. 1970, *Ap. J.*, **162**, 791.
- Sato, C. 1980, *Publ. Astron. Soc. Jap.*, **32**, 41.
- Spitzer, L. Jr., and Saslaw, W. C., 1966, *Ap. J.*, **143**, 400.
- Strom, R. G. 1988, *M. N. R. A. S.*, **230**, 331.
- Taylor, J. H., and Dewey, R. J. 1988, *Ap. J.*, **332**, 770.
- Taylor, J. H., and Weisberg, J. M. 1989, *Ap. J.*, **345**, 434.

- Tonry, J. L. 1989, in *Dynamics of Dense Stellar Systems*, ed. D. Merritt (Cambridge: Cambridge University Press), p. 35.
- van der Marel, R. P., de Zeeuw, P. T., Rix, H. W., and Quinlan, G. D. 1997, *Nature*, **385**, 610.
- Weidemann, V. 1990, *Ann. Rev. Astron. Astrophys.*, **28**, 103.
- Woosley, S. E., and Weaver, T. A. 1986, *Ann. Rev. Astron. Astrophys.*, **24**, 205.
- Young, P. 1980, *Ap. J.***242**, 1232.

Table 1. Four Galactic and Magellanic black hole candidates.

candidate	lower mass limit (M_{\odot})	probable mass (M_{\odot})
Cygnus X-1	6	16 ± 5
LMC X-3	3	> 9
LMC X-1	4	7 ± 3
0620-00	3	> 7.3

Table 2. Initial model parameters for the simulations in this study.

Model	c/a	N	IMF/ M_{\odot}	range/ M_{\odot}	★ evo.	★ col.	★ for.	$\frac{t_{col}}{t_{rel}}$	M_{\bullet}/M
Group 1									
XVIa	1.0	300	$\delta(m-1)$	1	n	y	n	100	0
XVIb	0.9	300	$\delta(m-1)$	1	n	y	n	100	0
XVIc	0.8	300	$\delta(m-1)$	1	n	y	n	100	0
XVI d	0.7	300	$\delta(m-1)$	1	n	y	n	100	0
XVIe	0.6	300	$\delta(m-1)$	1	n	y	n	100	0
XVIf	0.5	300	$\delta(m-1)$	1	n	y	n	100	0
XVIg	0.4	300	$\delta(m-1)$	1	n	y	n	100	0
XVIh	0.3	300	$\delta(m-1)$	1	n	y	n	100	0
Group 2									
IX	1.0	3000	$\delta(m-1)$	1	y	y	n	100	0
X	0.3	3000	$\delta(m-1)$	1	y	y	n	100	0
XI	1.0	3000	$\delta(m-1)$	1	y	y	n	100	0.1
XII	0.3	3000	$\delta(m-1)$	1	y	y	n	100	0.1
Group 3									
XIIIa	0.8	3000	$m^{-2.35}$	[0.2,1]	y	y	n	100	0
XIIIb	0.8	1000	$m^{-2.35}$	[0.2,1]	y	y	n	100	0
XIIIc	0.8	300	$m^{-2.35}$	[0.2,1]	y	y	n	100	0
XIII d	0.8	100	$m^{-2.35}$	[0.2,1]	y	y	n	100	0
XIIIe	0.8	30	$m^{-2.35}$	[0.2,1]	y	y	n	100	0
XIVa	0.8	3000	$m^{-2.35}$	[0.2,1]	y	y	n	100	0.1
XIVb	0.8	1000	$m^{-2.35}$	[0.2,1]	n	n	n	100	0.1
XV	0.8	3000	$m^{-2.35}$	[0.2,1]	y	y	y	100	0
XVII	0.8	3000	$m^{-2.35}$	[0.2,1]	n	n	n	100	0
XVIII	0.8	3000	$m^{-2.35}$	[0.2,1]	y	y	y	10	0

Table 3. Dominant merger remnants produced in a selection of the simulations.

model	N/2	★ evo.	★ col.	★ for.	m_{rem}/M_{\odot}	ϵ
IX	1500	yes	yes	no	3.0	0.00200
X	1500	yes	yes	no	5.0	0.00333
XI	1500	yes	yes	no	8.0	0.00533
XII	1500	yes	yes	no	10.0	0.00667
XV	1500	yes	yes	yes	4.1	0.00271
XVIg	150	no	yes	no	43.0	0.287
XIIIa	1500	yes	yes	no	2.7	0.00160
XIIIb	500	yes	yes	no	2.8	0.00560
XIIIc	150	yes	yes	no	2.4	0.0160
XIIId	50	yes	yes	no	2.2	0.0440
XIIIe	15	yes	yes	no	1.9	0.0380

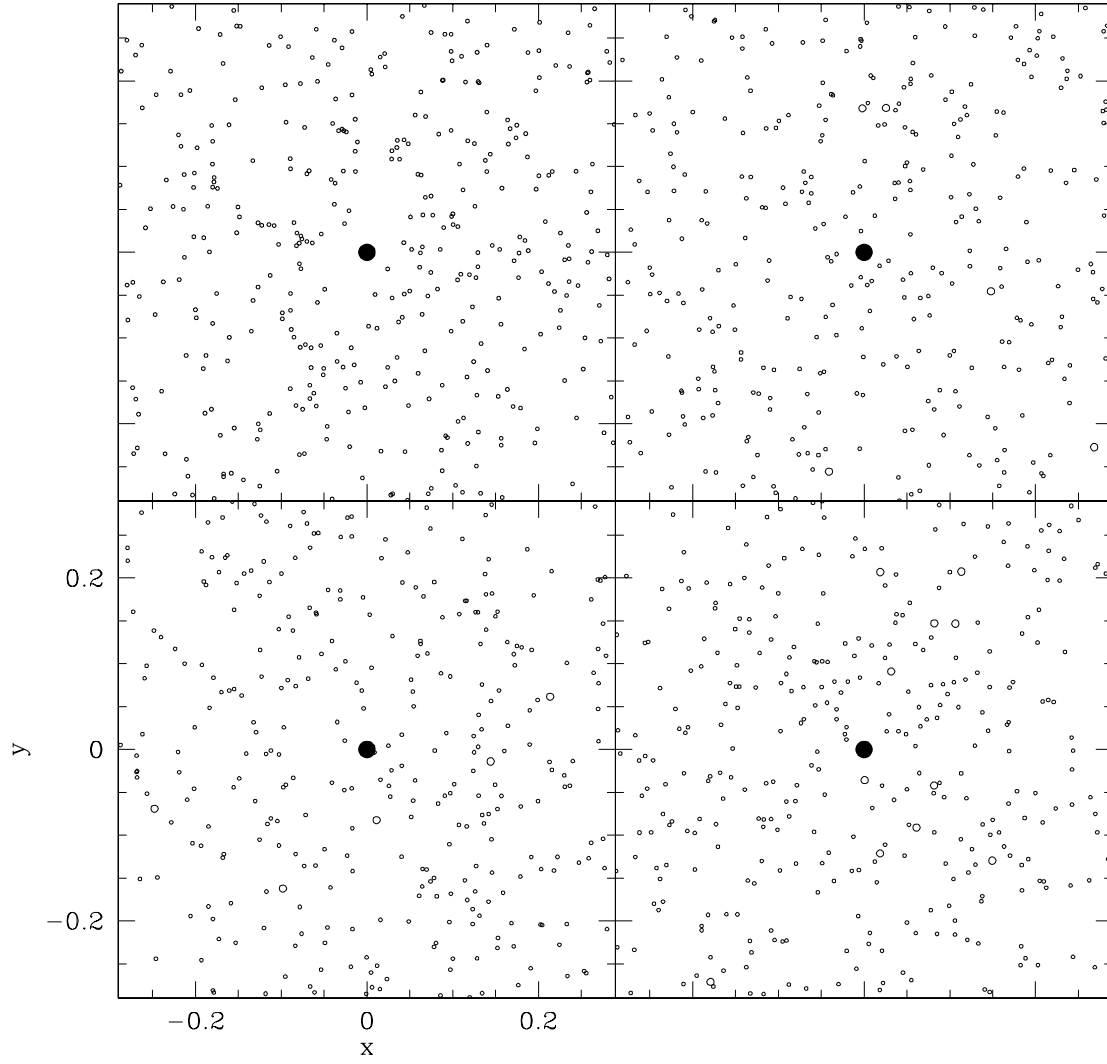


Fig. 1.— The early evolution of the central region of a spherical system containing a black hole (model XI; see Table 2) at $t/t_{rc} = 0, 1, 2$, and 3.

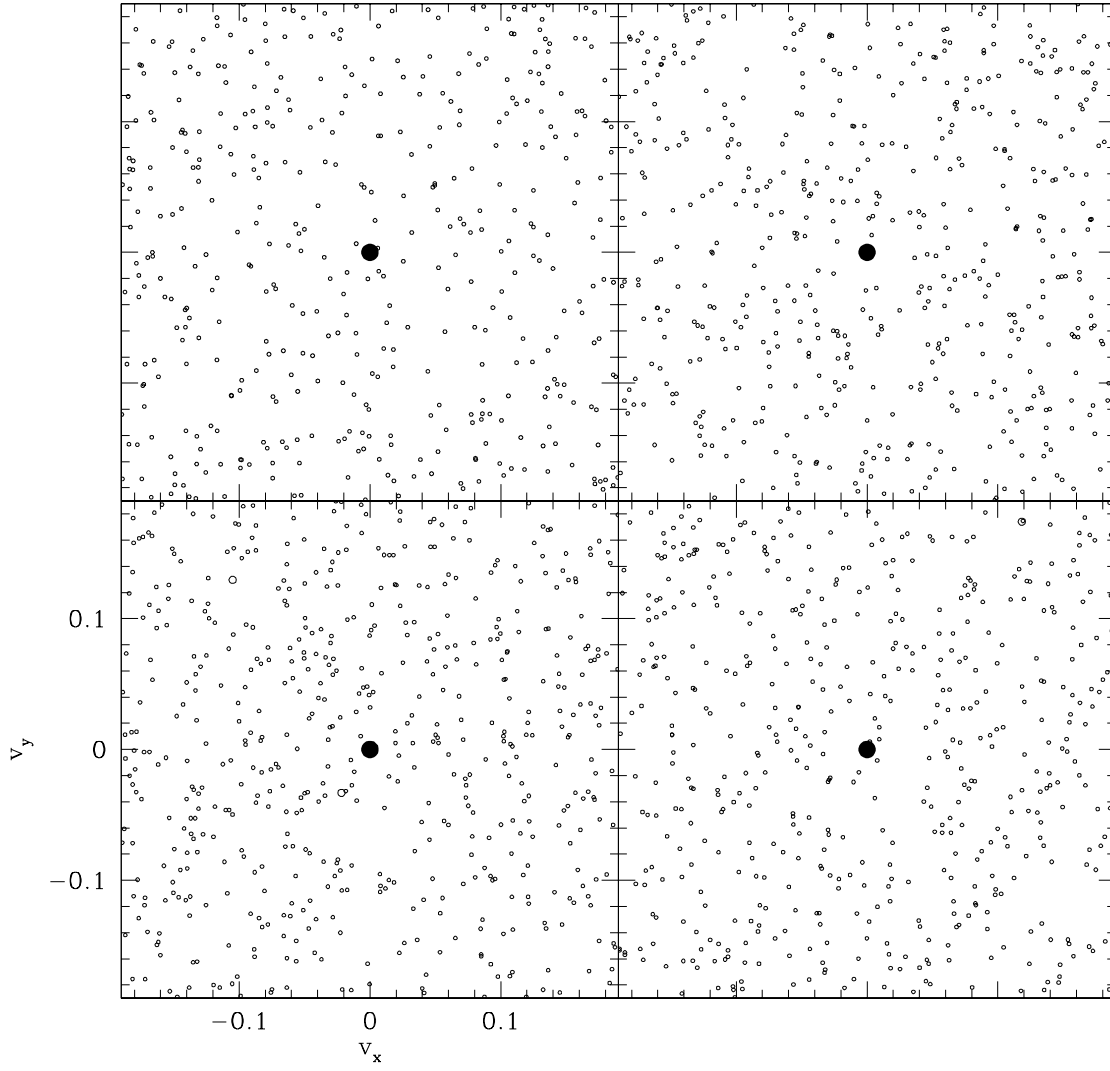


Fig. 2.— The early velocity evolution of the center of a spherical system containing a black hole (model XI; see Table 2) at $t/t_{rc} = 0, 1, 2,$ and 3 .

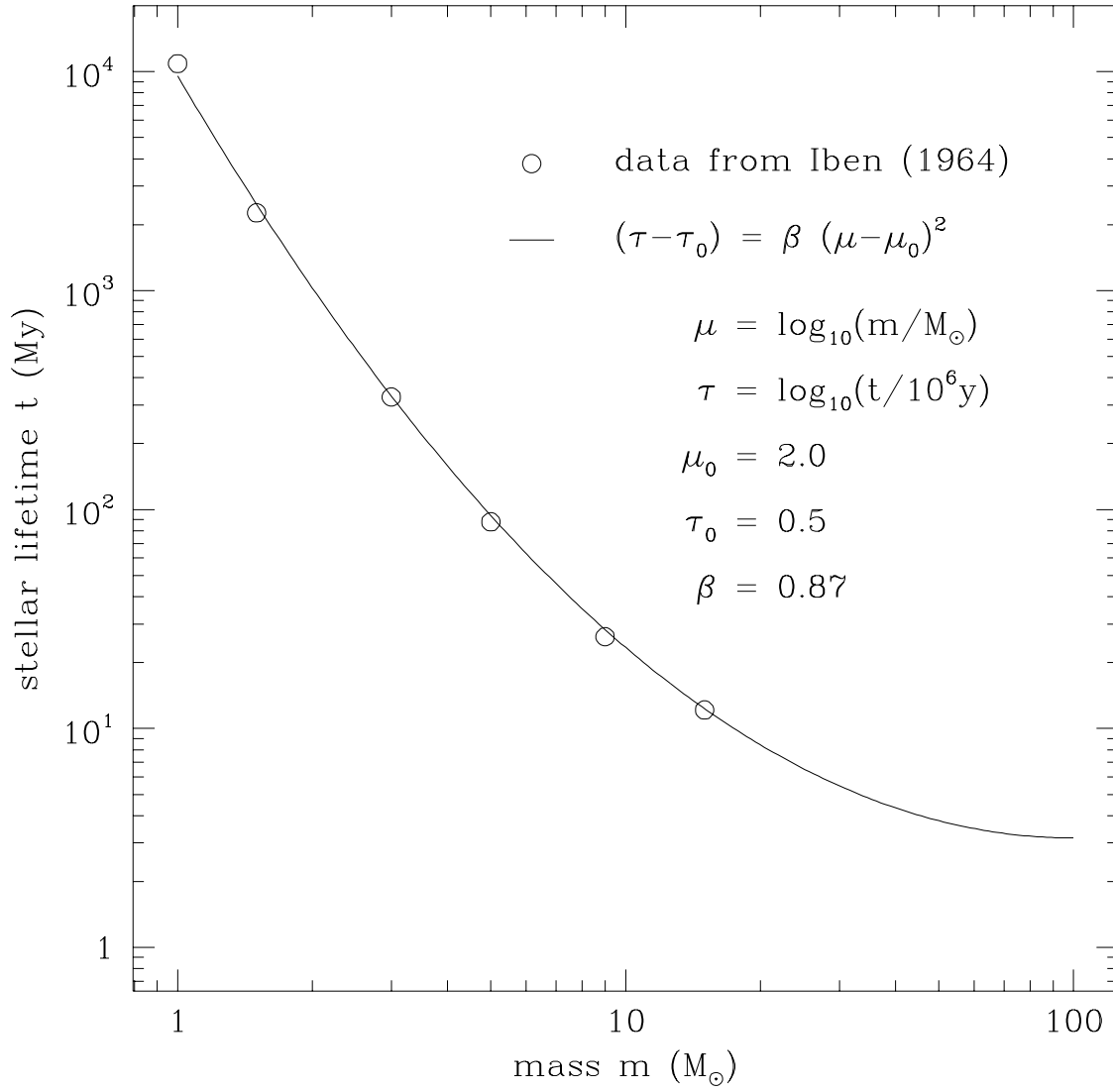


Fig. 3.— Main sequence life time versus mass for stars in simulations incorporating stellar evolution effects.

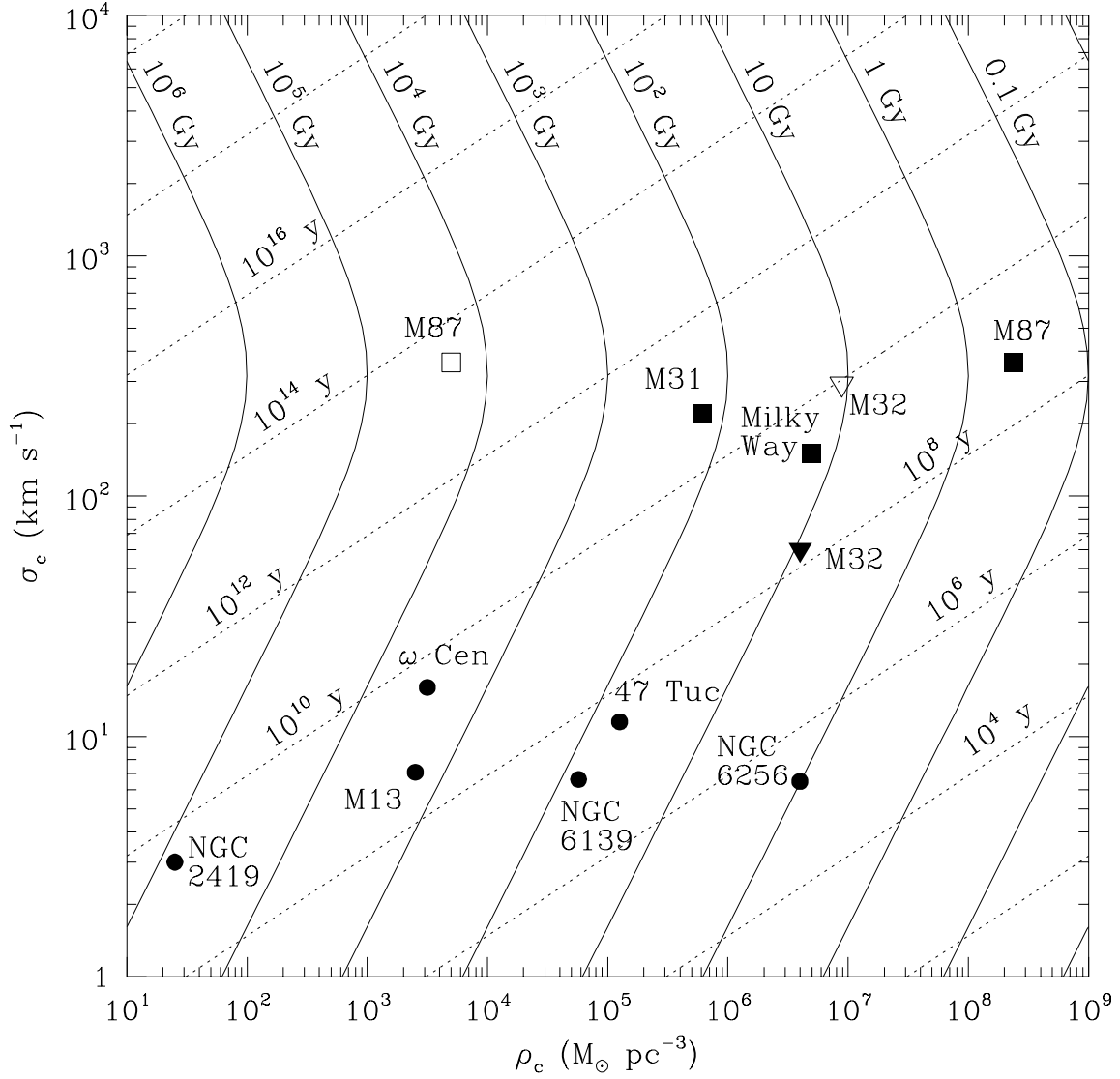


Fig. 4.— Stellar collision (solid) and relaxation (dashed) time scale contours for a large range of core dispersion and density. The cores of several local stellar systems are included.

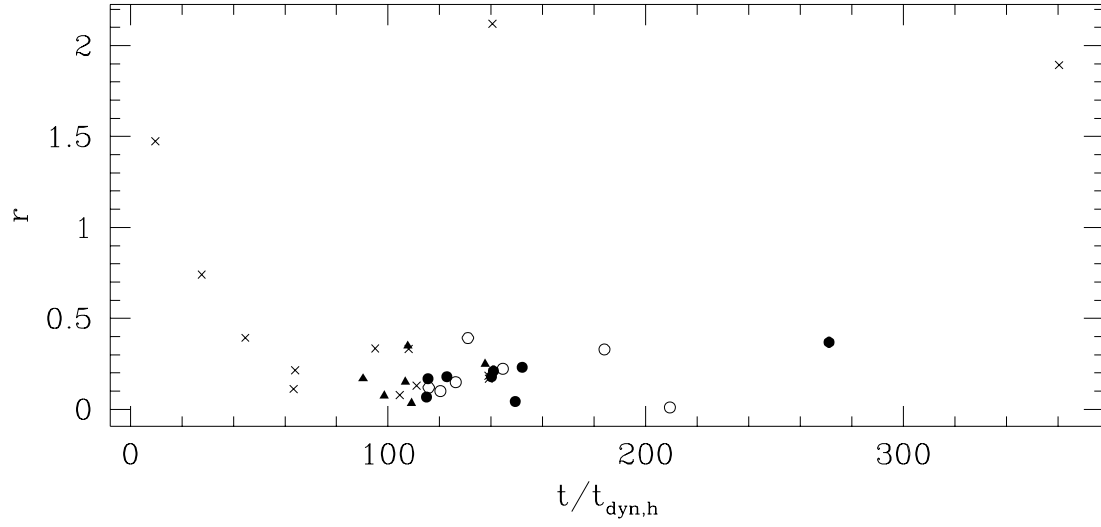


Fig. 5.— Center of mass distance of collision events for spherical model XVIa.

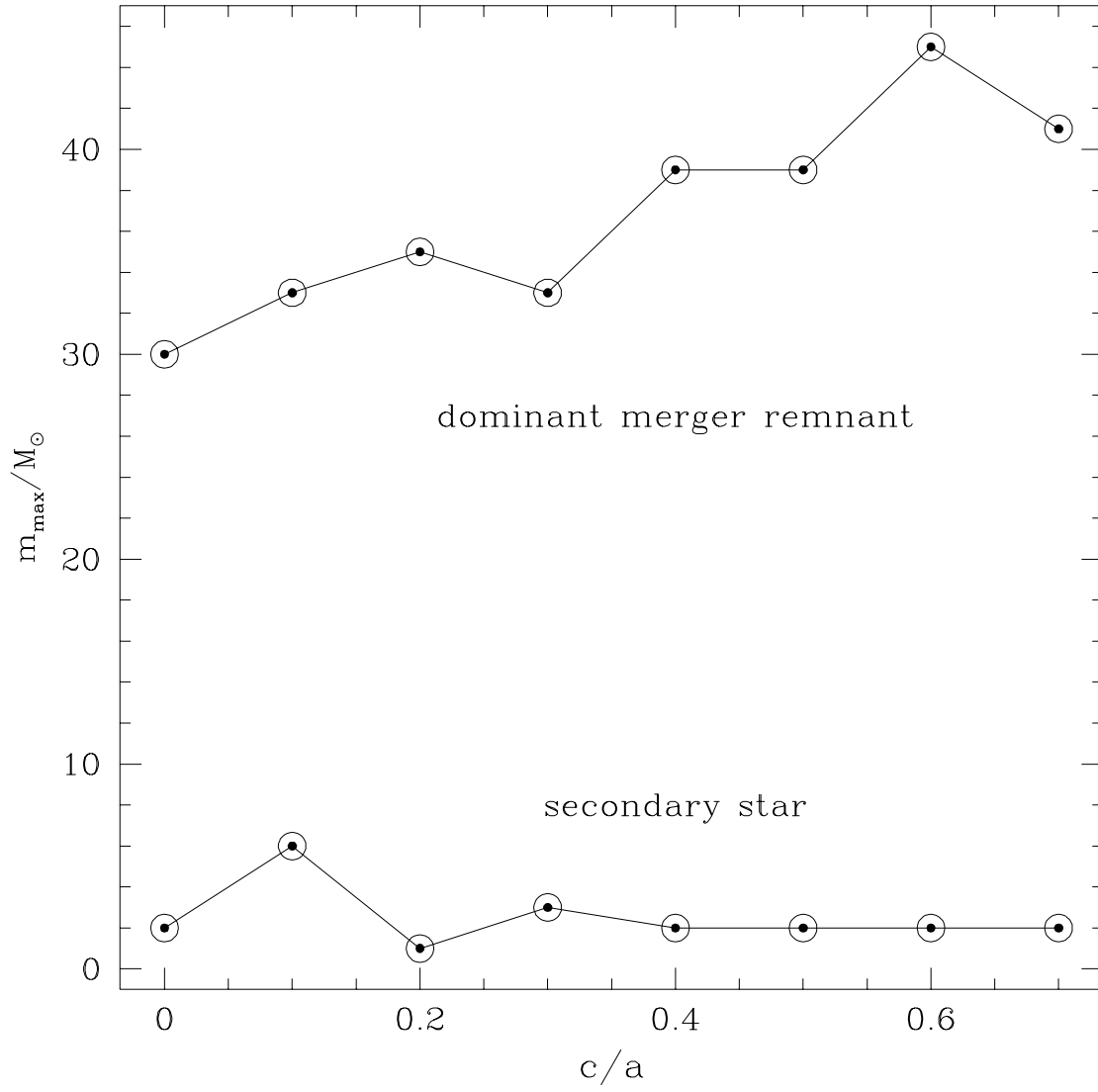


Fig. 6.— Dominant merger remnant mass and secondary star mass as a function of the initial KK model axial ratio.

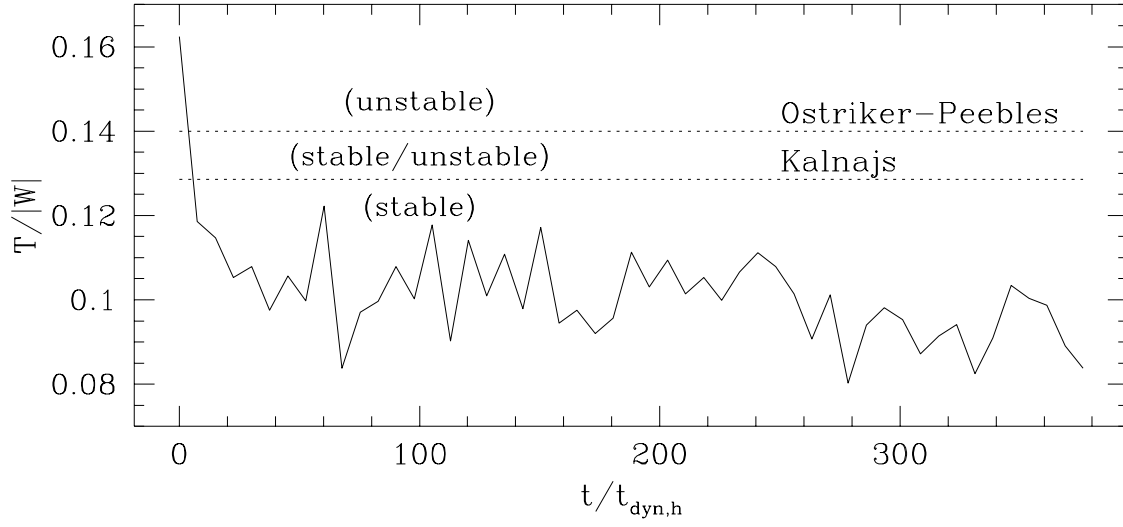


Fig. 7.— The $T/|W|$ evolution of model XVIIh ($c/a = 0.3$, 300 equal-mass stars).

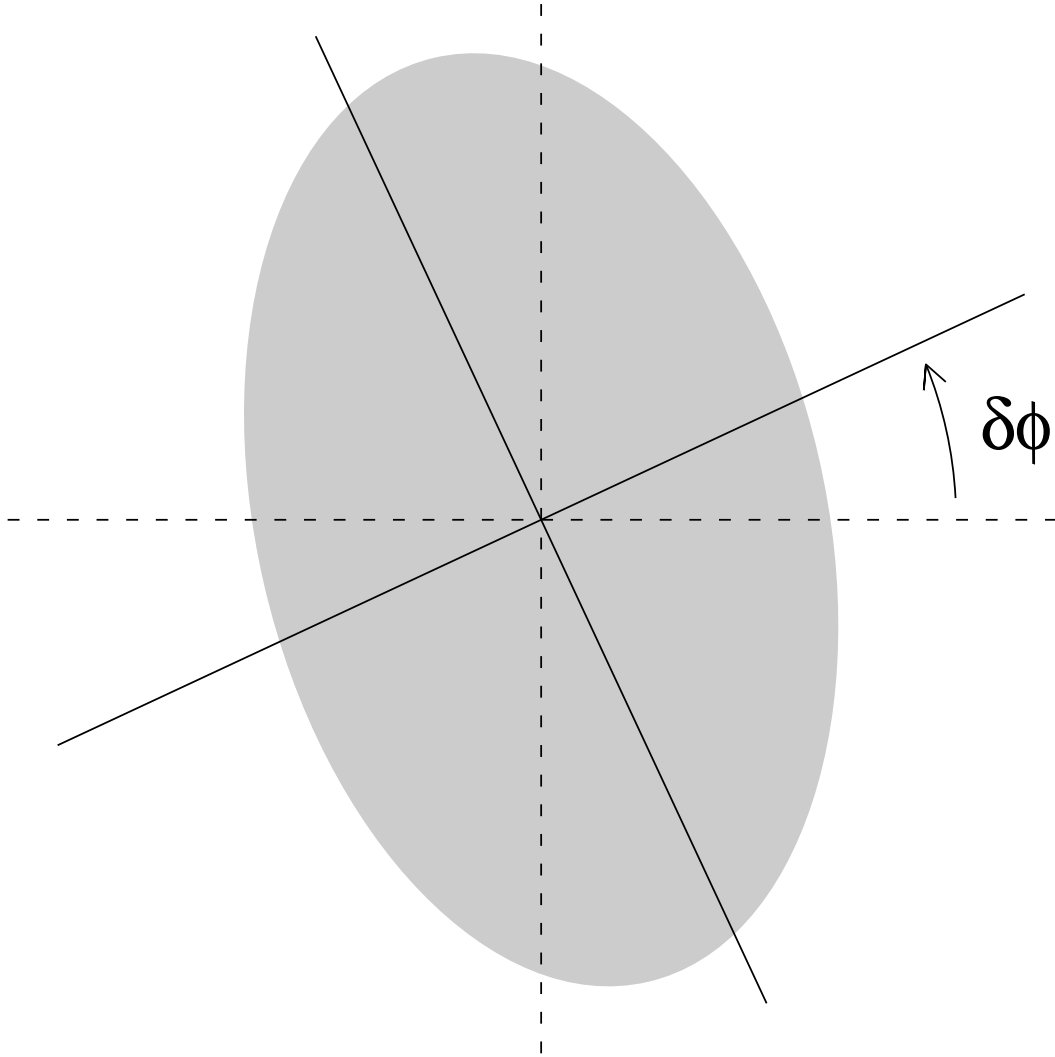


Fig. 8.— Geometry for identifying the bar structure of a low-N system.

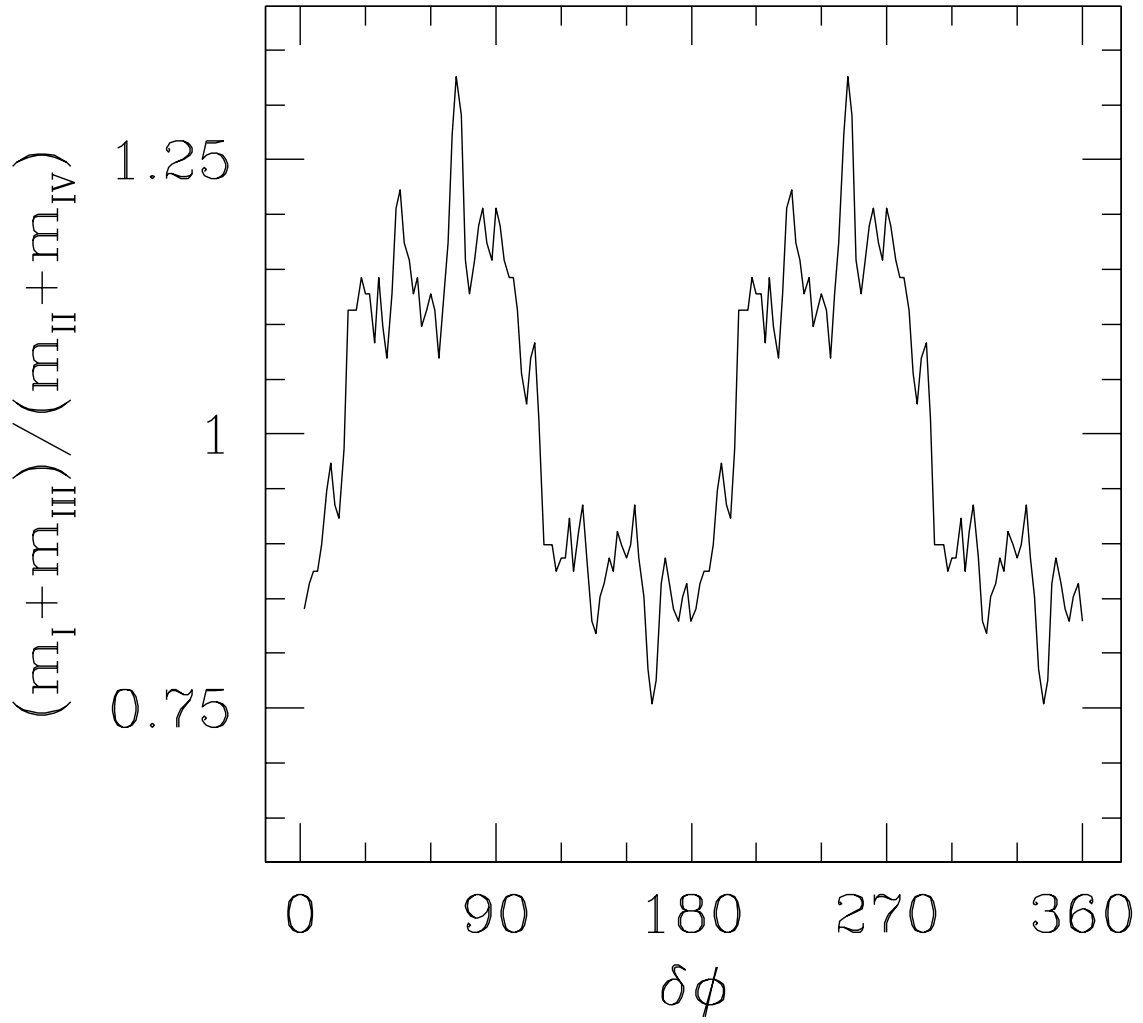


Fig. 9.— The ratio of opposite-quadrant mass sums as a function of axial offset for model XVIIh.

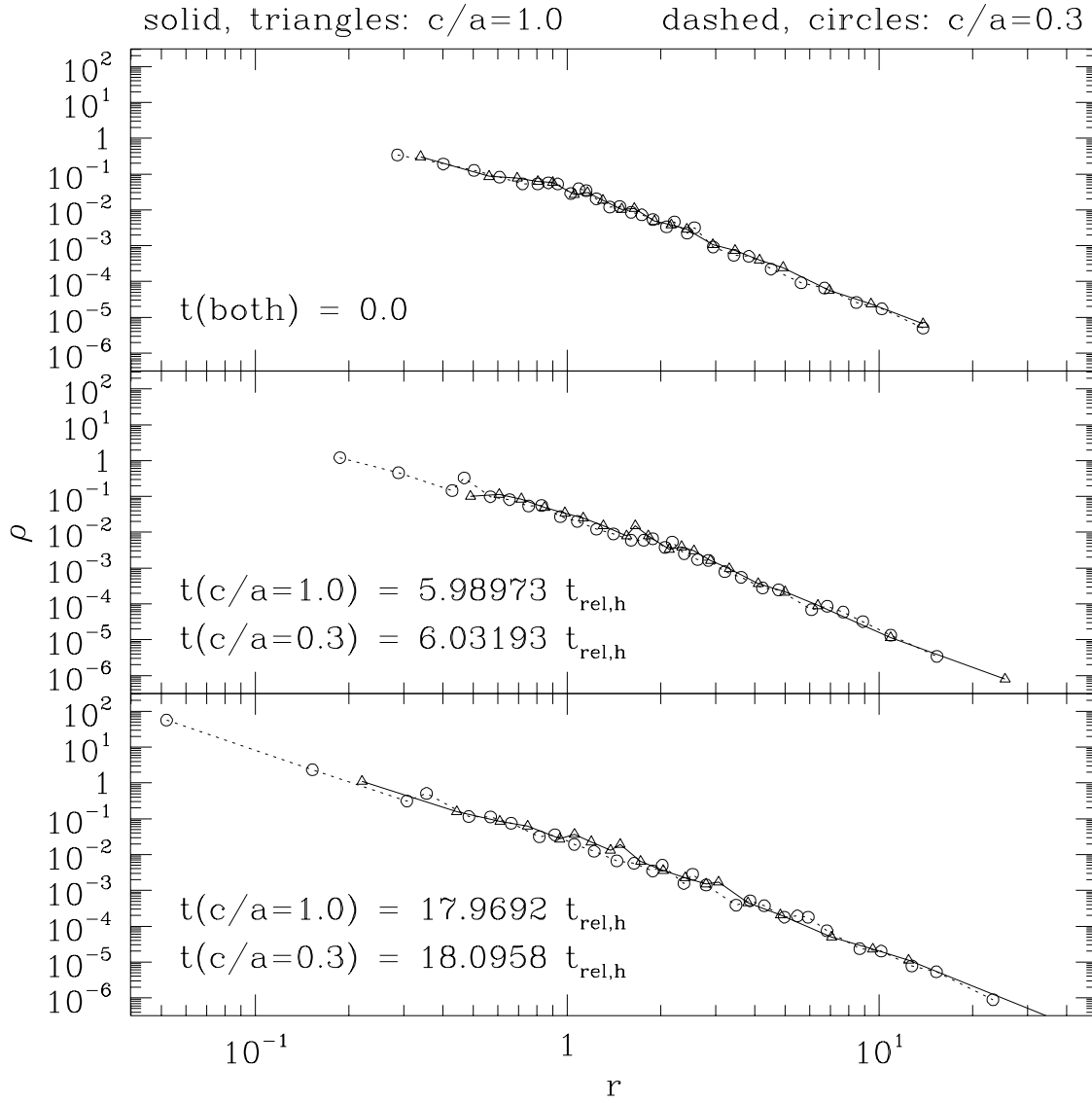


Fig. 10.— Density profiles for the spherical and the flattest Group 1 systems. Note that the times given are in units of the initial half-mass relaxation time scale.

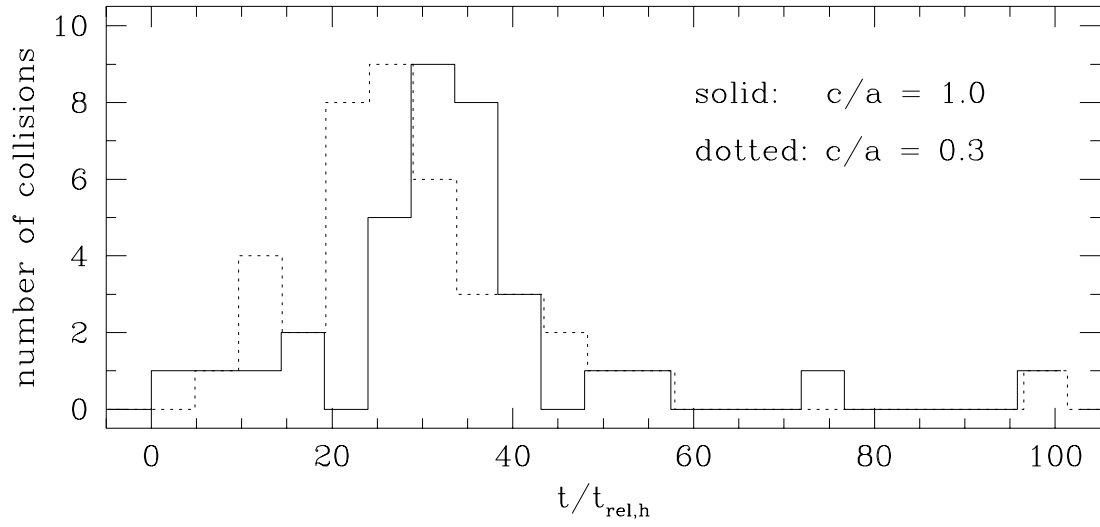


Fig. 11.— Collision rate for the spherical and the flattest Group 1 simulations.

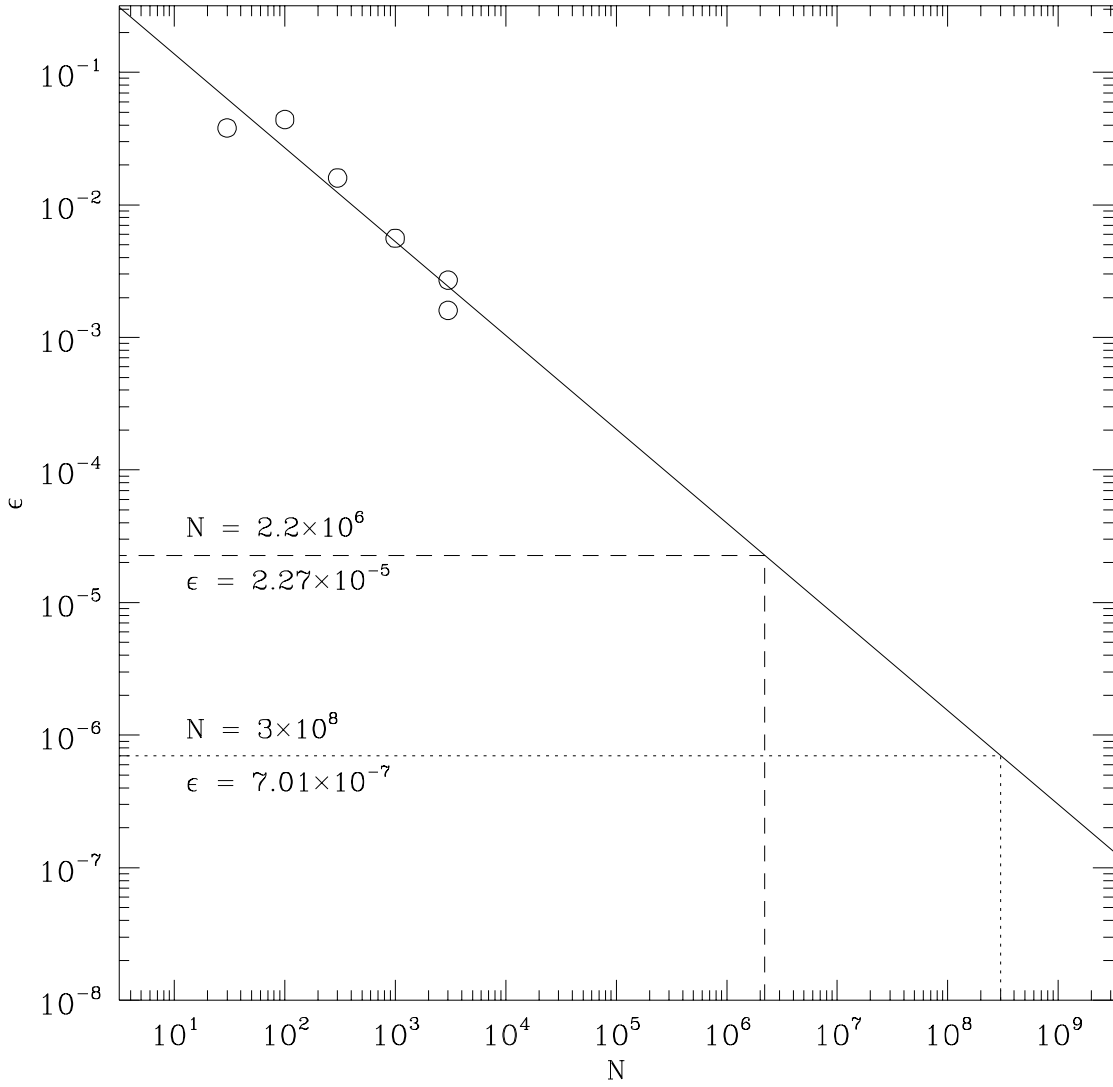


Fig. 12.— The stellar merger efficiencies of models XIII and XV. The power law fit to the points has a slope of -0.708 and an intercept of -0.155.

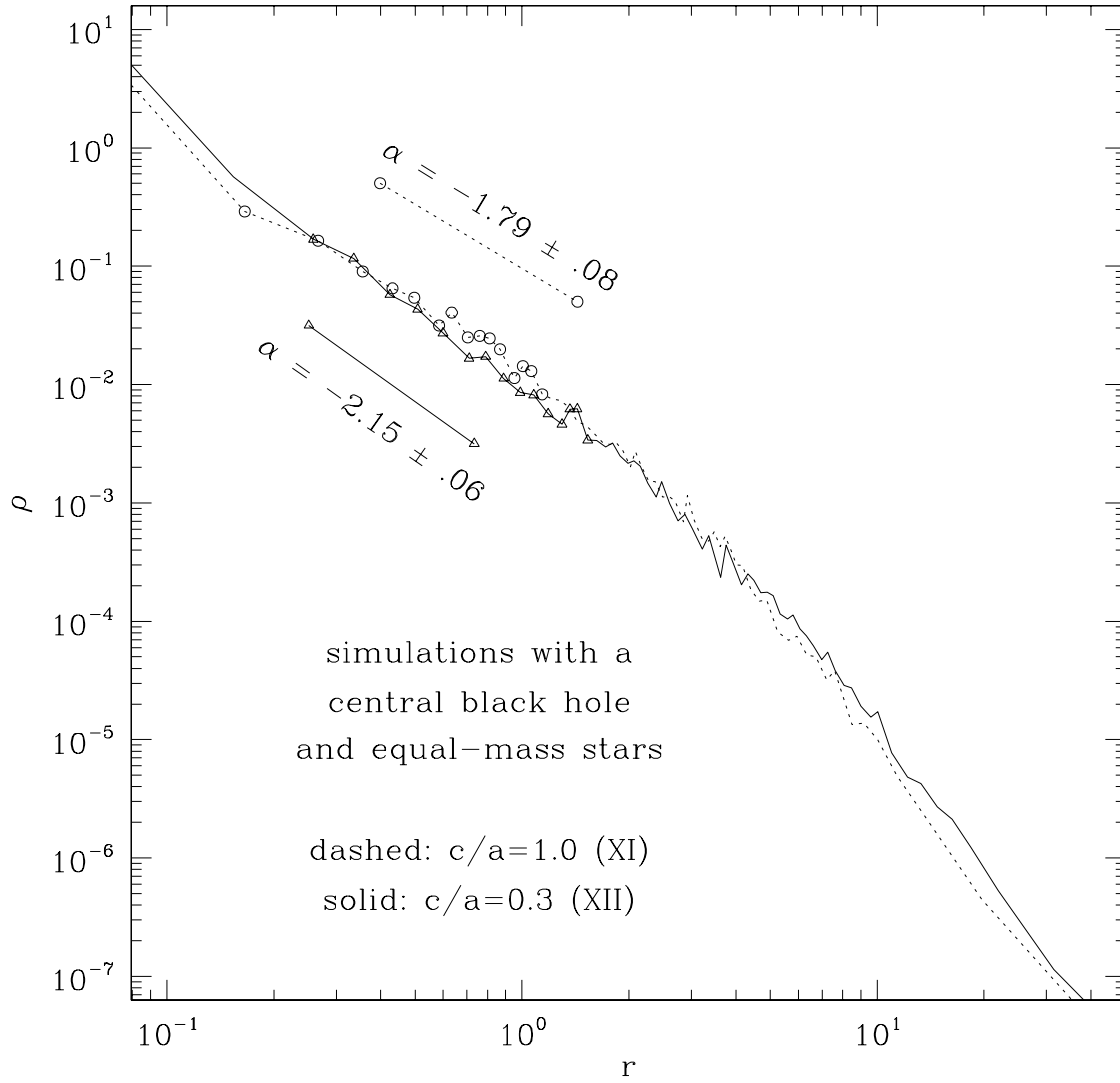


Fig. 13.— Density profiles for simulations containing a central black hole and equal-mass stars. The dashed line is a spherical model (XI) and the solid line is rotationally flattened (XII).

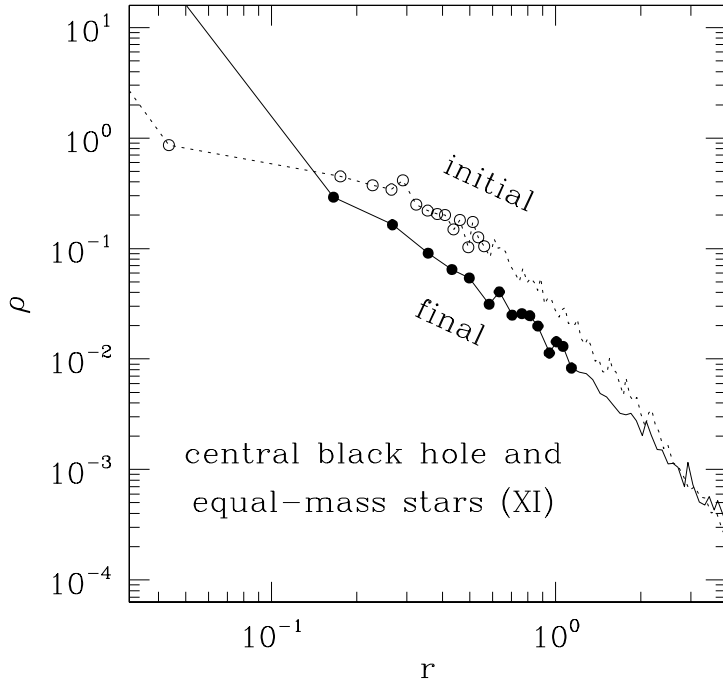


Fig. 14.— Initial and final density profiles of model XI.

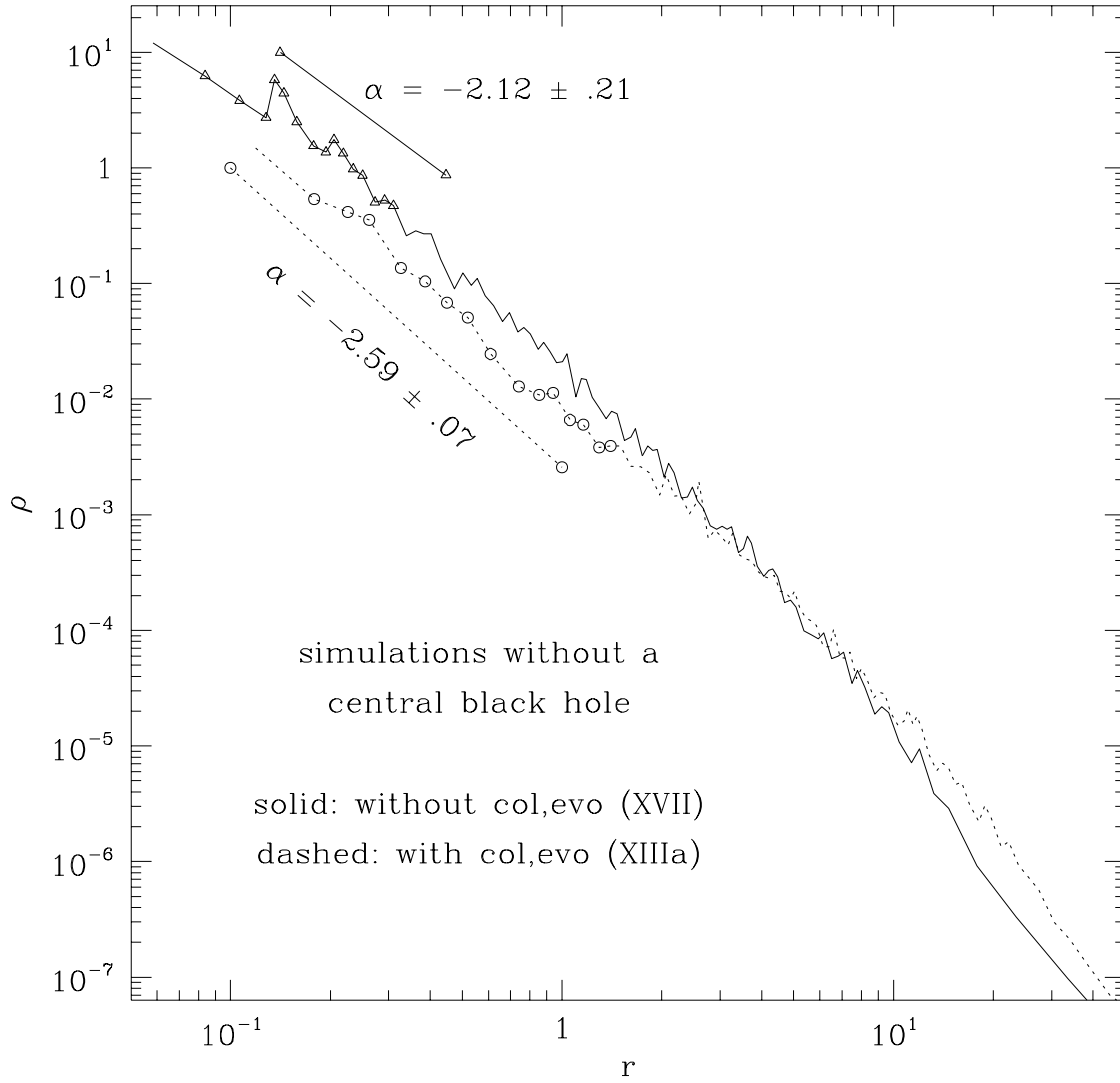


Fig. 15.— Density profiles for Salpeter IMF $c/a = 0.8$ simulations without central black holes.

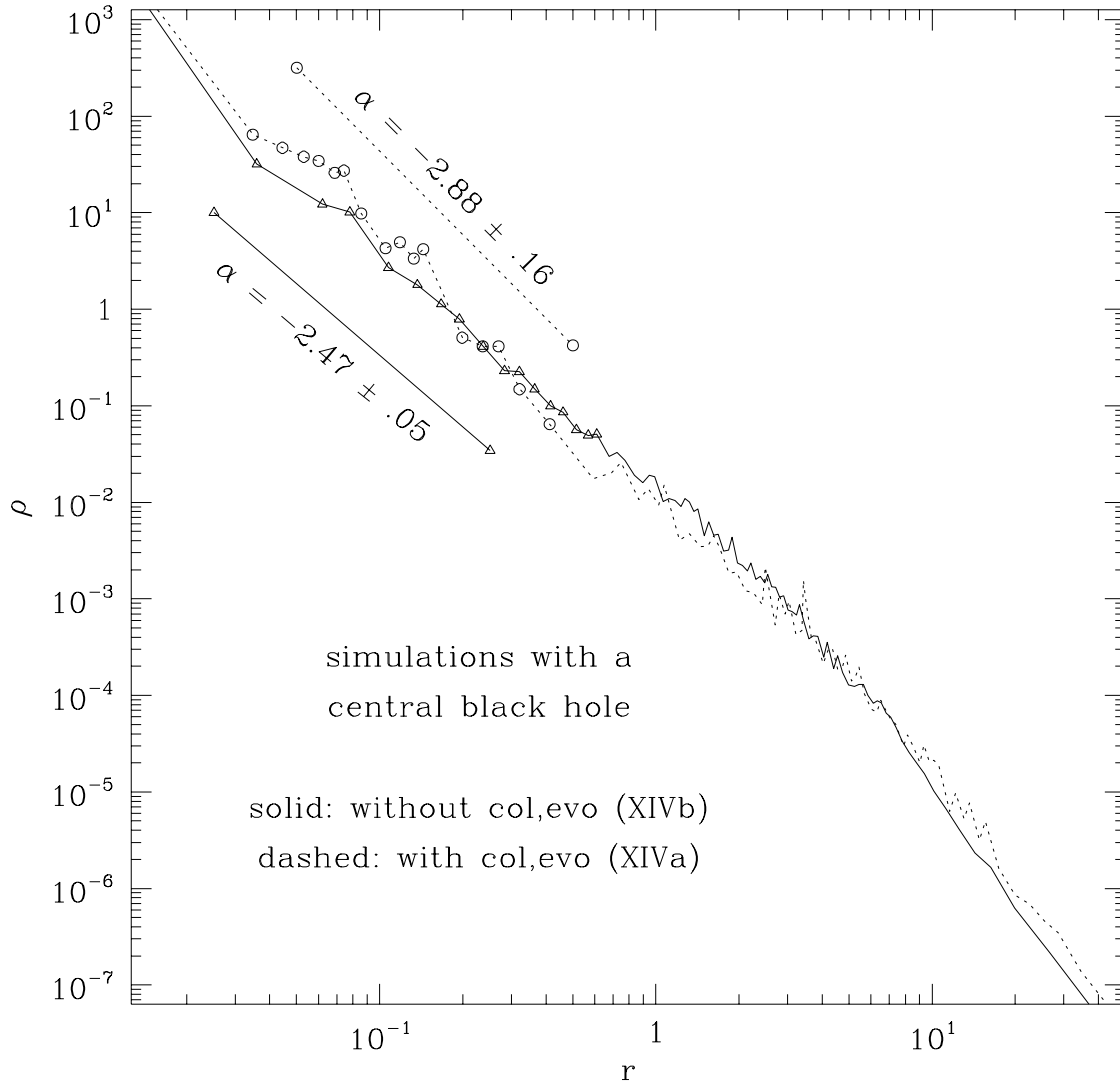


Fig. 16.— Density profiles for Salpeter IMF $c/a = 0.8$ simulations with central black holes.

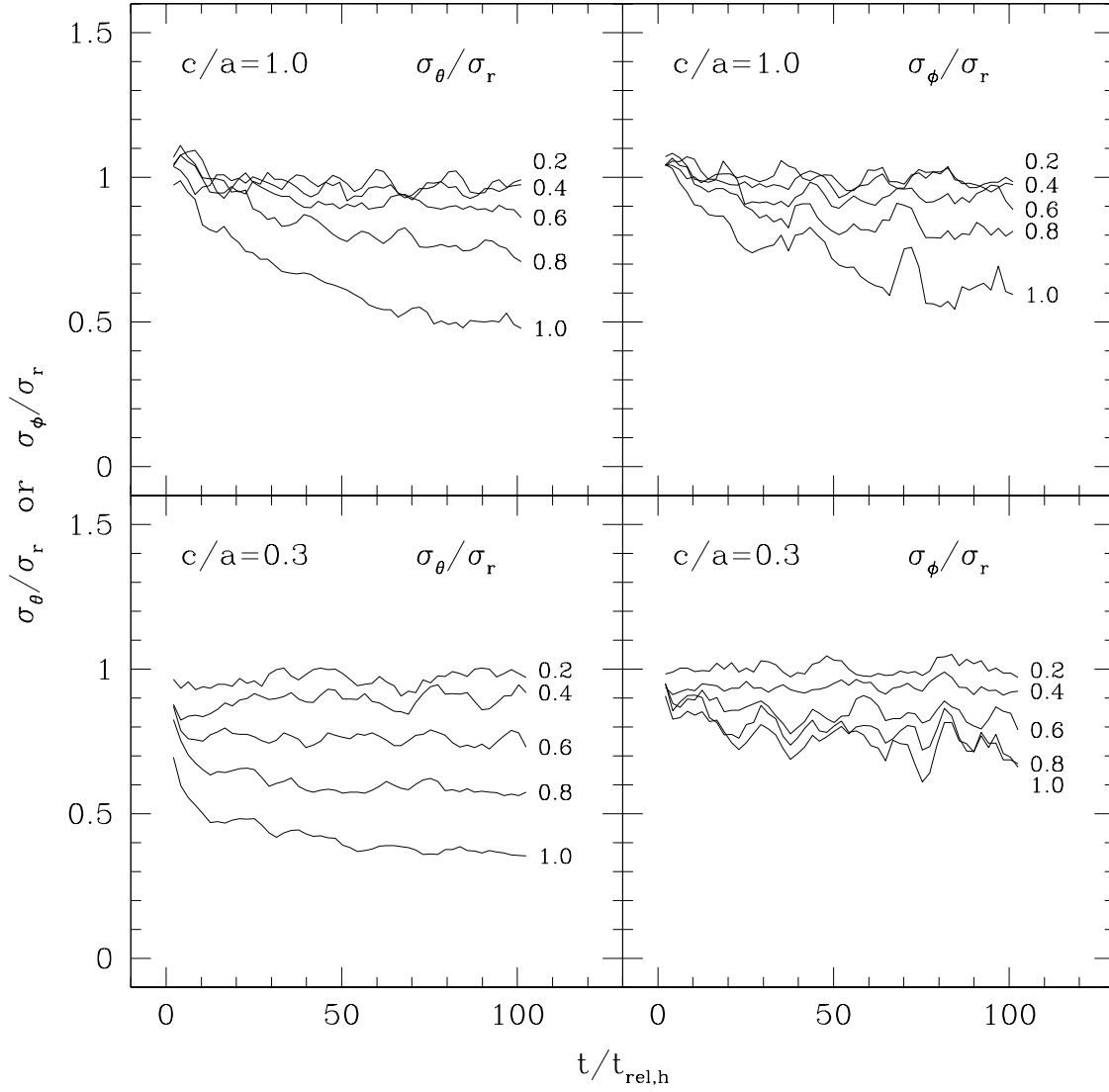


Fig. 17.— Developing radial anisotropy in models which contain no central black hole, for two different rotational states (IX and X).

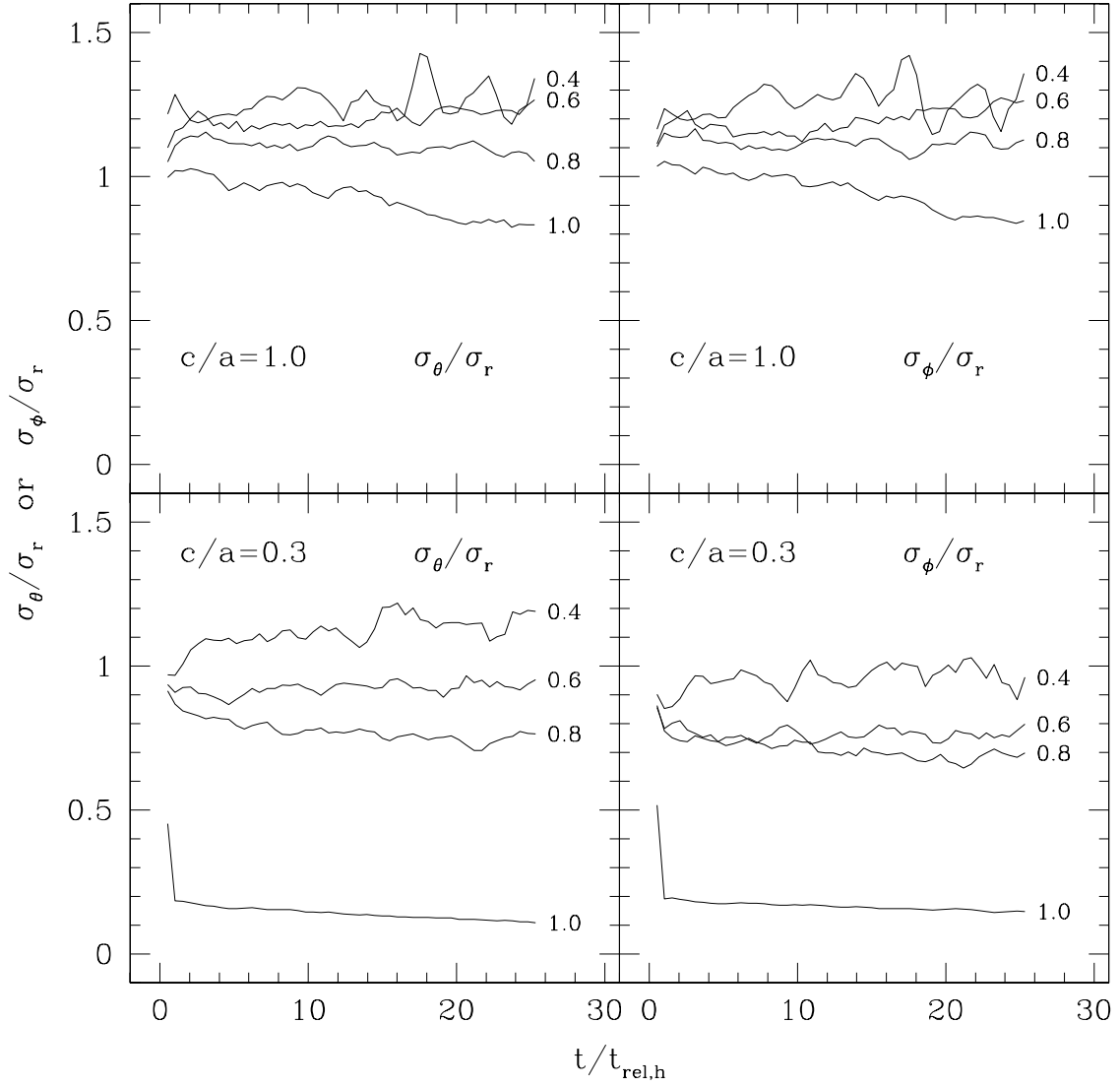


Fig. 18.— Developing anisotropy in models XI and XII (equal-mass stars with a central black hole).

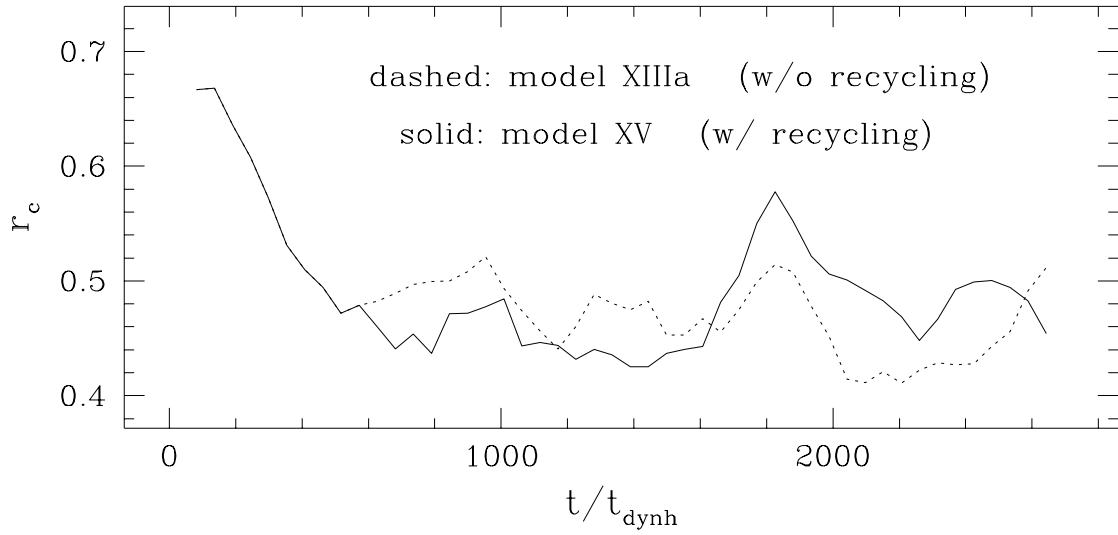


Fig. 19.— Comparison of core radius evolution between systems which do (XV) and do not (XIIIa) recycle stellar ejecta into new stars.

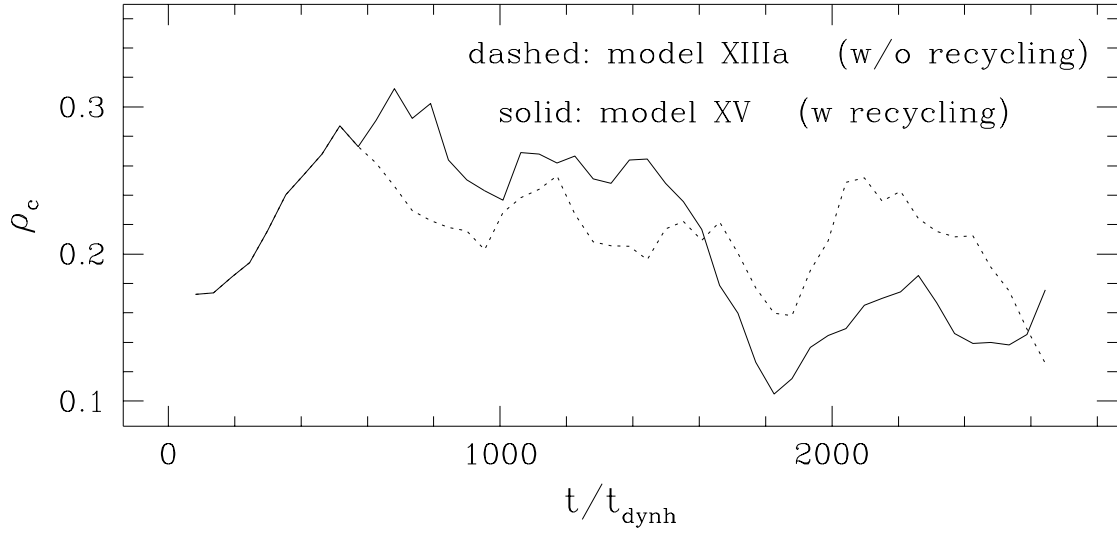


Fig. 20.— Comparison of core density evolution between systems which do and do not recycle stellar ejecta into new stars.

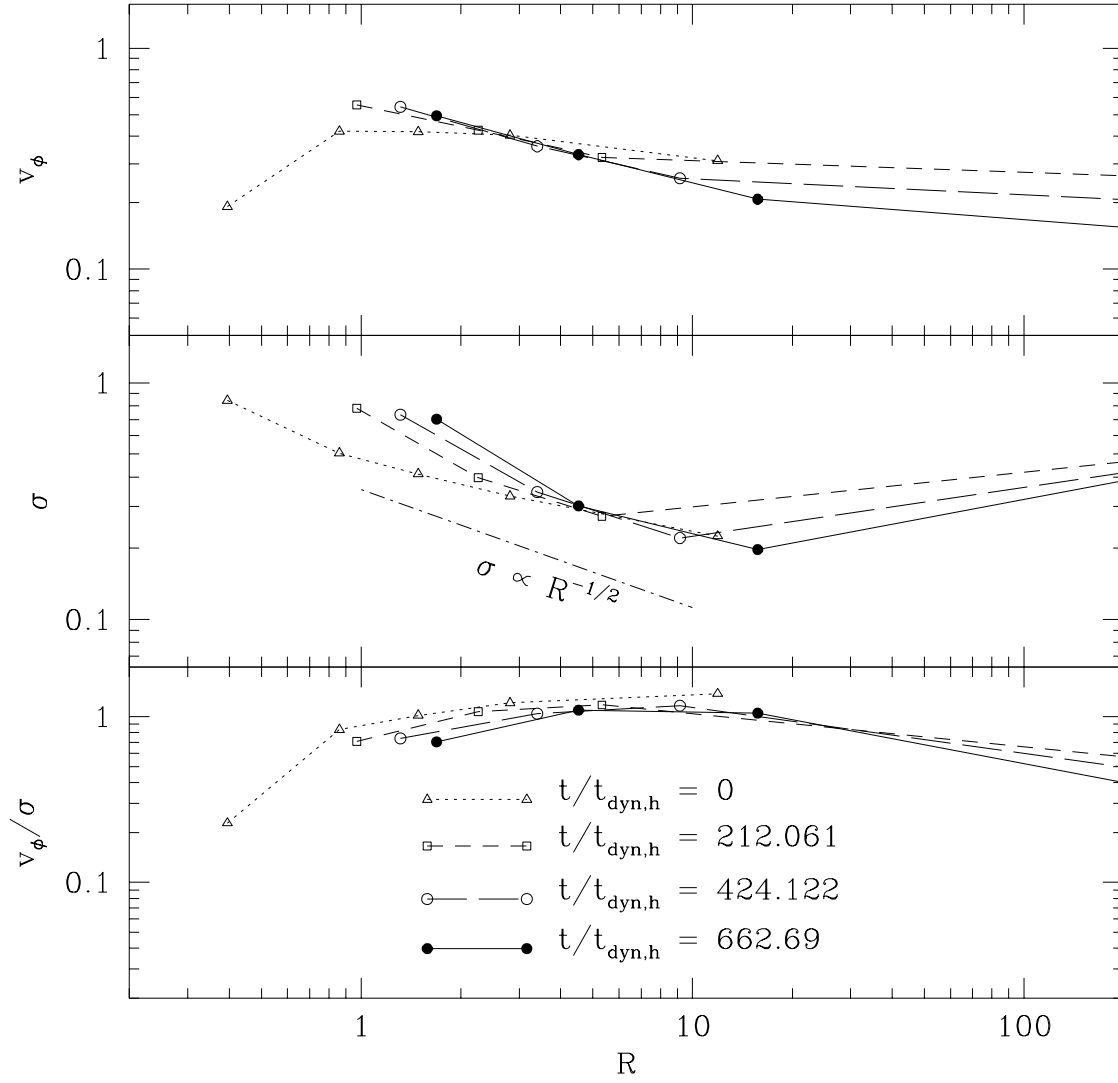


Fig. 21.— Rotation-related properties of model XII (equal-mass stars with a central black hole).